Title

The kinesin KIF4 mediates HBV/HDV entry through regulation of surface NTCP localization and can be targeted by RXR agonists *in vitro*.

Running title

KIF4 regulates NTCP-mediated HBV/HDV entry

Authors

Sameh A. Gad[1,2,3], Masaya Sugiyama[4], Masataka Tsuge[5], Kosho Wakae[1], Kento Fukano[1], Mizuki Oshima[1,6], Camille Sureau[7], Noriyuki Watanabe[1], Takanobu Kato[1], Asako Murayama[1], Yingfang Li[1], Ikuo Shoji[8], Kunitada Shimotohno[9], Kazuaki Chayama[10,11,12], Masamichi Muramatsu[1], Takaji Wakita[1], Tomoyoshi Nozaki[2], Hussein H. Aly[1]

Affiliation

[1]Department of Virology II, National Institute of Infectious Diseases, 1-23-1 Toyama, Shinjuku-ku, Tokyo 162-8640, Japan
[2]Department of Biomedical Chemistry, Graduate School of Medicine, The University of Tokyo, Tokyo 113-0033, Japan
[3]Department of Microbiology and Immunology, Faculty of Pharmacy, Minia University, Minia 61519, Egypt
[4]Genome Medical Sciences Project, National Center for Global Health and Medicine, 1-7-1 Kohnodai, Ichikawa, Chiba, 272-8516, Japan
[5]Natural Science Center for Basic Research and Development, Hiroshima University, 1-2-3 Kasumi, Minami-ku, Hiroshima, 734-8551, Japan
[6]Graduate School of Science and Technology, Tokyo University of Science, Noda 278-8510, Japan
[7]Institut National de la Transfusion Sanguine, Paris, 6 rue Alexandre Cabanel, 75739 Paris, France
[8]Center for Infectious Diseases, Kobe University Graduate School of Medicine, 7-5-1 Kusunoki-cho, Chuo-ku Kobe 650-0017, Japan
[9]Center for Hepatitis and Immunology, National Center for Global Health and Medicine, Chiba 272-8516, Japan
[10]Collaborative Research Laboratory of Medical Innovation, Graduate School of Biomedical and Health Sciences, Hiroshima University, 1-2-3, Kasumi, Minami-ku, Hiroshima-shi, Hiroshima, 734-8551 Japan
[11]Research Center for Hepatology and Gastroenterology, Graduate School of Biomedical and Health Sciences, Hiroshima University, Hiroshima, Japan.
[12]RIKEN Center for Integrative Medical Sciences, Yokohama, Japan.

Corresponding Authors

Hussein H. Aly, email: ahussein@nih.go.jp; Takaji Wakita, email: wakita@nih.go.jp

The word count for the abstract: 250 words

The word count for the text: 4885 words

Abstract

Intracellular transport via microtubule-based dynein and kinesin family motors plays a key role in viral reproduction and transmission. We show here that Kinesin Family Member 4 (KIF4) plays an important role in HBV/HDV infection. We intended to explore host factors impacting the HBV life cycle that can be therapeutically addressed using siRNA library transfection and HBV/NLuc (HBV/NL) reporter virus infection in HepG2-hNTCP C4 cells. KIF4 silencing resulted in a 3-fold reduction in luciferase activity following HBV/NL infection and suppressed both wild-type HBV and HDV infection. Transient KIF4 depletion reduced surface and raised intracellular NTCP (HBV/HDV entry receptor) levels, according to both cellular fractionation and immunofluorescence analysis (IF). Overexpression of wild-type KIF4 but not ATPase-null KIF4 regains the surface localization of NTCP in these cells. Furthermore, immunofluorescence (IF) revealed KIF4 and NTCP colocalization across microtubule filaments, and a co-immunoprecipitation study showed that KIF4 physically binds to NTCP. KIF4 expression is regulated by FOXM1. Interestingly, we discovered that RXR agonists (Bexarotene, and Alitretinoin) down-regulated KIF4 expression via FOXM1-mediated suppression, resulting in a substantial decrease in HBV-Pre-S1 protein attachment to HepG2-hNTCP cell surface and subsequent suppression of HBV infection in HepG2-hNTCP and primary

human hepatocytes (PXB) (Bexarotene, IC_{50} 1.89 ± 0.98 μM). Overall, our findings show that human KIF4 is a critical regulator of NTCP surface transport and localization, which is required for NTCP to function as a receptor for HBV/HDV entry. Furthermore, small molecules that suppress or alleviate KIF4 expression would be potential antiviral candidates that target HBV and HDV entry phases.

Author Summary

Understanding HBV/HDV entry machinery and the mechanism by which NTCP (HBV/HDV entry receptor) surface expression is regulated is crucial to develop antiviral entry inhibitors. We found that NTCP surface transport is mainly controlled by the motor kinesin KIF4. Surprisingly, KIF4 was negatively regulated by RXR receptors through FOXM1-mediated suppression

This study not only mechanistically correlated the role of RXR receptors in regulating HBV/HDV entry but also suggested a novel approach to develop therapeutic rexinoids for preventing HBV and/or HDV infections in important clinical situations, such as in patients undergoing liver transplantation or those who are at a high risk of HBV infection and unresponsive to HBV vaccination.

77

78 ## Introduction

79 Hepatitis B virus (HBV) affects about 250 million individuals globally and is a major
80 cause of chronic liver inflammation. Cirrhosis, liver failure, and liver cancer can all result
81 from a protracted condition of hepatic inflammation and regeneration (1). Sodium
82 taurocholate cotransporting polypeptide (NTCP) was discovered in 2012 to be a key
83 cellular receptor for HBV and its satellite hepatitis delta virus (HDV), which shares the
84 same envelope as HBV (2, 3). When HBV nucleocapsid infects human hepatocytes, it is
85 carried to the nucleus, where the partially double-stranded rcDNA genome is repaired to
86 covalently closed circular (ccc) DNA. This episomal DNA acts as a template for all viral
87 transcripts and pregenomic RNA, forming a very stable minichromosome that is the
88 primary cause of chronic HBV infection, the generation of antiviral escape mutants, or
89 relapse after ceasing nucleo(t)ide analog anti-HBV treatment (4).

90 Kinesins are a vast protein superfamily that is responsible for the movement of
91 numerous cargos within cells such as membrane organelles, mRNAs, intermediate
92 filaments, and signaling molecules along microtubules (5). Kinesins are also thought to
93 regulate cell division, cell motility, spindle assembly, and chromosomal
94 alignment/segregation (6, 7). KIF4 is a highly conserved member of kinesin family (8-
95 10). KIF4 is also known to move to the nucleus during mitosis, where it interacts with

96 chromatin to alter spindle length and control cytokinesis (11). KIF4A has previously been
97 shown to improve the transport of HIV and adenovirus capsids early in infection (12, 13).
98 As a result, KIF4A might be a promising antiviral target. The transcriptional activator
99 Forkhead box M1 (FOXM1) has been shown to increase KIF4A expression in
100 hepatocellular carcinoma (HCC) (14). Interestingly, HBV upregulates KIF4 expression
101 in HepG2 hepatoma cells, and it was reported to be considerably higher in HBV-
102 associated liver malignancies (15); no information on the role of KIF4 in HBV infection
103 is currently known.

104 We performed functional siRNA screening using an HBV reporter virus and HepG2-
105 hNTCP cells to uncover host factors that impact the HBV life cycle. We identified KIF4
106 as a positive regulator for the early phases of HBV/HDV infection based on the findings
107 of this screen. Further investigation indicated that KIF4 is a critical component in the
108 transport and surface localization of NTCP, where it can function as a receptor for
109 HBV/HDV entry. RXR agonists like Bexarotene reduced KIF4 expression and
110 HBV/HDV infection by targeting FOXM1. This is the first study to show that KIF4 plays
111 an essential role in HBV/HDV entry and that it may be used to build effective anti-HBV
112 entry inhibitors.

113

Results

KIF4 is a proviral host factor required for the early stages of HBV infection

We previously used HBV particles containing a chimeric HBV genome (HBV/NL), in which HBV core region is substituted by NanoLuc (NL) gene, to infect HepG2-hNTCP cells formerly transfected with a druggable genome siRNA library two days before HBV/NL infection. We looked at 2,200 human genes to see if they had any effect on the HBV life cycle (16). HBV/NL does not replicate because the HBV core protein (HBc) is not expressed, and the NL levels released after infection only represent the early phases of HBV infection, from the entry through transcription of HBV pregenomic RNA (pgRNA). For each plate, nontargeting or anti-NTCP siRNAs were employed as controls (Fig. 1A). The XTT (2,3-bis-[2-methoxy-4-nitro-5-sulfophenyl]-2H-tetrazolium-5-carboxanilide) test was used to assess cell viability; wells with ≥20% loss of cell viability were removed from further investigation. Previously, we discovered host factors with anti-HBV action (16). In this paper, we describe the discovery of new host factors (proviral factors) necessary in the early stages of HBV infection. The independent silencing of just 14 of the 2,200 host genes (0.6%) reduced NL activity by more than 70% (average of three distinct siRNAs) (Fig. 1B). These genes were identified as pro-HBV host factors (NTCP, SAT1, DVL3, AOX1, DGKH, CAMK1D, CHEK2, AK3, ROCK2,

RYK, KIF4, TFIP11, SLC39A6, MXRA5). KIF4 was previously shown to be induced in vitro by HBV expression *in vitro* (15). We also looked at data from an accessible database (17) and discovered that KIF4 was expressed at considerably greater levels in patients with persistent HBV infection than in healthy people ($P < 0.001$). (Fig. 1C). The role of KIF4 in HBV life cycle is not yet reported, hence, we performed further investigation to clarify it. Silencing KIF4 expression with two distinct siRNA sequences (Fig. 1E) led to a 2-fold ($P < 0.001$) or 3-fold ($P < 0.001$) reduction in NL activity relative to cells transfected with the control siRNA (Fig. 1D).

KIF4 is required for cell culture-derived HBV (HBVcc) infection

We used authentic HBV particles generated from grown HepAD38.7-Tet cells to validate the relevance of KIF4 in the HBV life cycle (HBVcc). We reduced KIF4 expression in HepG2-hNTCP cells by transfecting particular siRNA 72 hours before HBVcc infection (Fig. 2A); after 10 to 13 days post infection (pi), we examined its influence on hepatitis B surface antigen (HBsAg), DNA, and HBc levels. As a positive control, si-NTCP was utilized. Silencing KIF4 expression resulted in a substantial decrease of HBsAg in the culture supernatant ($P < 0.001$) to levels equivalent to silencing NTCP expression (Fig. 2B). siKIF4 also decreased overall HBV-DNA levels as measured by southern blot (Fig. 2C) and inhibited HBc expression as measured by

150 immunofluorescence (IF) (Fig. 2D) to levels equivalent to si-NTCP without
151 compromising cellular viability (Fig. 2E). We employed primary human hepatocytes
152 (PXB) cells to examine the effect of suppressing KIF4 expression on HBV infection in a
153 more physiologically relevant paradigm (Fig. 2F). As predicted, inhibiting KIF4 or NTCP
154 expression dramatically reduced HBs levels by ELISA ($P < 0.01$) (Fig. 2G) and decreased
155 extracellular HBV-DNA levels by real-time PCR ($P < 0.001$). (Fig. 2H). Figure 2I depicts
156 the silencing efficiency of KIF4 siRNA in PXB cells.

157 **KIF4 regulates HBV and HDV entry into host cells**

158 Then, using particular siRNA, we suppressed KIF4 expression and examined the stage
159 of the HBV life cycle that is controlled by KIF4. NTCP plays a role in the specific binding
160 of HBV to the host cell surface by interacting with the preS1 region of HBV's large
161 surface protein (LHB) (3). We investigated the attachment of a fluorescence-labeled
162 preS1 peptide (6-carboxytetramethylrhodamine-labeled preS1 peptide, or TAMRA-
163 preS1) to HepG2-hNTCP (Fig. 3A). The preS1 binding assay was conducted with si-
164 NTCP as a positive control to validate the specificity of the observed TAMRA-preS1
165 signals. KIF4 silencing dramatically reduced the interaction between TAMRA-labeled
166 PreS1 and NTCP as identified by IF (Fig. 3A, left pictures) and shown by signal
167 intensities (Fig. 3A, right panel). These findings support the notion that KIF4 is essential

for the interaction of HBV and surface NTCP. Using a luciferase reporter system for the various HBV promoters, we discovered that KIF4 expression did not influence the transcriptional activity of these promoters (Fig. 3B). Furthermore, utilizing HBV replicon cells, HepAD38.7-Tet off, which produce HBV pgRNA following tetracycline withdrawal, we discovered that suppressing KIF4 expression did not influence intracellular HBV-DNA levels. (See Fig. 3C.) HDV has the same envelope as HBV and utilizes NTCP as a receptor to enter hepatocytes (2). Consistent with the results obtained in the HBV infection and preS1-binding tests, suppressing KIF4 expression reduced HDV susceptibility in NTCP-expressing cells (Fig. 3D, left pictures), and the magnitude of KIF4 siRNA suppression on HDV infection is displayed in Fig. 3D, right panel. These findings show that KIF4 primarily controlled NTCP-mediated HBV and HDV entry into cells while having little or no influence on HBV transcription or replication.

KIF4 regulates surface NTCP expression

We investigated the influence of KIF4 on total and subcellular (both surface and cytoplasmic) NTCP expression after discovering that it is necessary for HBV entrance via regulating the interaction between HBV preS1 and NTCP. Silencing of KIF4 expression did not affect total cellular NTCP protein levels, as shown in figure 4A, but IF examination revealed that silencing of KIF4 disrupted NTCP surface localization and

encouraged its accumulation in the cytoplasm (Fig. 4B). This conclusion was supported by biochemical investigation, which indicated that silencing KIF4 dramatically decreased surface NTCP in membranous fraction (Fig. 4C) while increasing intracellular NTCP protein levels in the cytoplasmic fraction (Fig. 4D). Figure 4E depicts band densitometry. It is worth mentioning that silencing KIF4 did not influence surface cadherin or cytoplasmic GAPDH protein levels, indicating that KIF4 has a particular effect on NTCP surface localization.

KIF4 motor activity is required for surface NTCP expression

Kinesins, such as KIF4, are motor proteins that hydrolyze ATP to transport different molecules along microtubules (7). Because KIF4 is necessary for surface NTCP expression, we hypothesized that it may function as a transporter that delivers NTCP to the cell surface. As a result, we investigated the function of KIF4 ATPase activity in NTCP surface expression. The sequence of an ATPase-null KIF4 was previously described (18). (Fig. 5A). To mute endogenous KIF4 expression, we utilized a tailored siRNA sequence (si-KIF4 3′ UTR) that targeted the 3′ UTR region of the KIF4 transcript (19) and compensated for this suppression by transfecting plasmids expressing the Myc-tagged WT or ATPase-null KIF4 sequences. Because they lack the 3′ UTR of endogenous KIF4 transcripts, the mRNAs of these constructs are resistant to si-KIF4 3′ UTR. Cellular

fractionation revealed that the expression of WT or ATPase-null mutants did not affect surface cadherin (CHD-1) expression, as predicted. Surface NTCP levels are considerably enhanced when KIF4 depletion is compensated with WT, but not ATPase-null KIF4 protein (Fig. 5B). These findings were supported by IF analysis, which revealed significantly greater levels of surface NTCP when endogenous KIF4 silencing was compensated for by WT-KIF4, but not by ATPase-null KIF4 (Fig. 5C, upper panels) (Fig. 5C, lower panels). The si-KIF4 3′ UTR exhibited a substantial reduction of KIF4 by real-time RT-PCR and no cellular cytotoxicity as determined by the XTT assay (Fig. 5D and E). Overall, our findings indicated that KIF4 ATPase (motor) activity is necessary for NTCP surface expression (transport).

Physical interaction between KIF4 and NTCP

We hypothesized that direct contact between KIF4 and NTCP across the microtubules is necessary for KIF4 to transport NTCP to the cell surface. We transfected HepG2-hNTCP cells with Halo-tagged KIF4 and examined their intracellular colocalization. Interestingly, IF analysis revealed a significant colocalization between KIF4, NTCP, and α-tubulin (a microtubule marker) (Fig. 6A upper panels). Two distinct cross-sectional lines were constructed (Fig. 6A, center panels), and the colocalization signal intensities were also displayed along these regions of interest (Fig. 6A lower panel). Overlap of KIF4,

NTCP, and α-tubulin signal peaks indicated KIF4 and NTCP colocalization along microtubules. The co-immunoprecipitation study verified the direct interaction between KIF4 and NTCP. Myc-tagged KIF4 and HA-tagged NTCP expressing vectors were co-transfected into HEK293-FT cells. We only noticed NTCP co-immunoprecipitation when we used Myc antibody to pull down Myc-tagged KIF4, but not when we used control-IgG (Fig. 6B). Overall, our findings indicate that KIF4 binds to NTCP directly across microtubules in the cytoplasm and uses its ATPase motor domain to transport and transfer NTCP to the cell surface, where it may function as a receptor for HBV and HDV entry.

RXR agonists down-regulate KIF4 expression and block HBV entry by FOXM1 - mediated suppression

The transcription factor forkhead box M1 (FOXM1) has been shown to increase KIF4A expression (14) and is thus anticipated to affect surface NTCP expression and HBV entry into hepatocytes. Furthermore, retinoids including retinoid acid receptor (RAR) and retinoid X receptor (RXR) agonists were reported to decrease FOXM1 expression in human oral squamous cell carcinoma (20) and were anticipated to down-regulate its downstream KIF4 expression and, ultimately, HBV entry. To test this theory, we looked at how various retinoids affected the attachment of TAMRA-labeled preS1 peptide to cell surface NTCP in HepG2-hNTCP cells (Fig. 7A). The preS1 binding assay was done in

the presence of NTCP inhibitor, Myrcludex B, as a positive control to confirm the specificity of the observed TAMRA-preS1 signals (21). Interestingly, we discovered that Alitretinoin, a RAR/RXR agonist with potent RXR activity, and Bexarotene, a Pan-RXR agonist, significantly reduced TAMRA-labeled PreS1 binding to NTCP as indicated by IF (Fig. 7A); however, Pan-RAR, ATRA, and RARα-agonist, Tamibarotene, did not affect the preS1 probe binding. These findings indicate that RXR agonists selectively decreased surface NTCP localization and inhibited HBV/NTCP interaction. We then performed a cellular fractionation and found that while treatment with Bexarotene did not affect total NTCP expression (Input, Fig. 7B), it effectively suppressed the level of NTCP protein in the cell surface fraction (Fig. 7B). Bexarotene treatment of HepG2-hNTCP cells resulted in a significant reduction of both FOXM1 and KIF4 expression, supporting our hypothesis (Fig. 7C). Consequently, pretreatment with 10 μM Bexarotene dramatically decreased HBV/NL infection in HepG2-hNTCP cells ($P < 0.001$) (Fig. 7D) without altering cell viability (Fig. 7E).

Bexarotene pretreatment significantly suppressed HBV and HDV infections in primary human hepatocytes

Bexarotene pretreatment (Fig. 8A) significantly reduced susceptibility to HBV infection in primary human hepatocytes (a more realistic model of HBV infection) in a

dose-dependent decrease in secreted HBsAg levels ($P < 0.001$) (Fig. 8B); the 50% inhibitory concentration (IC_{50}) was estimated to be 1.89 ± 0.98 μM. Surprisingly, Bexarotene was not harmful to primary human hepatocyte cultures over a wide range of doses, with a 50% cytotoxic concentration (CC_{50}) of more than 50 μM. (Fig. 8C). Bexarotene's selectivity index (CC_{50}/IC_{50} ratio) was found to be > 26. We then changed the timing of Bexarotene administration in order to cover the different stages of HBV life cycle in primary human hepatocytes (Bexarotene was administered as follows: pre = 3 days before infection; co = during the inoculation of HBV particles from d0 to d1 pi; post = from d4 to d12 pi; and whole = from 3 days pre infection to d12 pi) (Fig. 8D). The expression of HBc protein by IF was used as a marker of HBV infection. While a modest suppression of HBc detection was found when Bexarotene is added co- or post- infection; the main suppressive effect of Bexarotene on the level of HBc protein was found when it was administered in (pre), or (whole) settings (Fig. 8E [immunofluorescence], and 8F [fluorescence intensity]). There was no apparent difference in Bexarotene-mediated suppression of HBc detection when it was administered in (pre) or (whole) settings. Since the administration of Bexarotene for 3 days before HBV infection is the common time frame between (pre) and (whole) settings, our data suggests that Bexarotene mainly exerts its suppression on HBV when administered before infection. This result is in line with our

finding that Bexarotene suppressed surface NTCP localization and subsequent HBV entry; hence its effect is mainly present when administered before (pre) infection. We investigated the effect of Bexarotene pretreatment on HDV infection since HDV has the same surface envelope and so employs NTCP to enter human hepatocytes. Bexarotene reduced HDV infection as predicted, as shown by a decrease in HDV RNA ($P < 0.001$). (Fig. 8G). These findings support the hypothesis that RXR agonists have a suppressive impact on HBV/HDV entry.

Discussion

The HBV/NL reporter system has previously been described to reflect the early phases of HBV infection (22). We previously reported using this method to screen 2200 druggable human genes and outlined the discovery of MafF and other host factors with anti-HBV function as a result of this screening (16). The current study describes the proviral host factors that are required for the early phases of HBV infection.

KIF4 belongs to the kinesin superfamily (KIFs). KIFs are ATP-dependent microtubule-based motor proteins that are involved in the intracellular transport (11). The N-terminal motor domain of KIF4 is in charge of ATP hydrolysis and microtubule-binding, whereas the C-terminal domain attaches to cargo molecules such as proteins, lipids, and nucleic

294 acids (23). We identified KIF4 as a pro-viral host factor required for the early phases of
295 HBV life cycle. The importance of KIF4 in boosting HBV infectivity early in the HBV
296 life cycle was verified in primary hepatocytes (Fig. 2).

297 The suppression of the interaction between HBV-PreS1 and HBV entry receptor
298 (surface NTCP) following silencing of KIF4 expression demonstrated the involvement of
299 KIF4 in regulating the function of NTCP as a receptor for HBV entry. HDV and HBV
300 share the same envelope proteins and hence rely on NTCP as an entry receptor into
301 hepatocytes (2). Silencing KIF4 expression dramatically reduced HDV infection, as
302 expected. KIF4 has previously been implicated in the anterograde transport of cellular
303 proteins such as Integrin beta-1 (24), as well as viral proteins such as retroviral (human
304 immunodeficiency virus (HIV-1), murine leukemia virus, Mason-Pfizer monkey virus,
305 and simian immunodeficiency virus) Gag polyprotein (25) to the cell surface to allow for
306 efficient retroviral particle formation. In line with KIF4's previously described
307 anterograde transport function, we discovered that inhibiting the ATPase motor activity
308 of KIF4 substantially reduced surface and raised cytoplasmic NTCP levels (Fig. 5). We
309 also used immunoprecipitation to validate the physical contact of KIF4 and NTCP, as
310 well as their colocalization on microtubules (Fig. 6). These findings demonstrated that
311 KIF4 controlled the anterograde transport of NTCP to the cell surface, influencing its

312 availability as a receptor for HBV/HDV entry on the hepatocyte surface.

313 Because the FOXM1 transcription factor is known to influence KIF4 expression (14)
314 it is predicted to affect surface NTCP expression and HBV internalization into
315 hepatocytes. Since retinoids, including RAR and RXR agonists, have been shown to
316 suppress FOXM1 expression in human oral squamous cell carcinoma (20), we
317 hypothesized that retinoid agonists would also suppress KIF4 expression, resulting in
318 impaired transport of NTCP to the cell surface and decreased susceptibility to HBV or
319 HDV infection. Only RXR agonists, Alitretinoin (26), and Bexarotene (27) decreased
320 HBV-PreS1 attachment to NTCP at the cell surface, indicating the specificity of RXR
321 agonists as HBV entry inhibitors (Fig. 7). Bexarotene, a pan-RXR agonist, substantially
322 decreased FOXM1, KIF4, and cell membrane-associated NTCP levels, which in turn
323 inhibited NTCP-dependent HBV-PreS1 binding to the cell surface and the consequent
324 HBV (IC_{50} 1.89 ± 0.98 μM) and/or HDV infection without any evident detrimental impact
325 in primary hepatocytes (Fig. 7) (Fig. 8).

326 This is the first research to describe Bexarotene as an HBV and HDV NTCP-mediated
327 entry inhibitor. Bexarotene has previously been shown to inhibit the early stages of HBV
328 infection when co-inoculated with HBV during the first 24 hours (28). This impact was
329 influenced in part by RXR-regulated gene expression in arachidonic acid

(AA)/eicosanoid biosynthesis pathways, which included the AA synthases phospholipase A2 group IIA (PLA2G2A). The specific step of the HBV life cycle (from attachment to cccDNA formation) impacted by Bexarotene was not defined in that study (28). Furthermore, silencing PLA2G2A expression marginally alleviated Bexarotene's inhibitory impact on HBV infection (28), indicating the presence of other key Bexarotene-dependent mechanisms that are still inhibiting the early stages of HBV infection. In line with that study, we found that co-treatment of Bexarotene with HBV inoculation moderately suppressed HBV infection, however, we also showed that the major suppression of HBV infection was obtained when Bexarotene was administrated pre-infection (Fig. 8E and F) suggesting the presence of other significant mechanism by which Bexarotene exerts its suppressive effect on HBV infection. Furthermore, we found that Bexarotene administration effectively suppressed surface NTCP levels (Fig. 7B). Hence, our data clearly showed that the main mechanism by which Bexarotene suppressed HBV infection is through the downregulation of surface NTCP levels prior to HBV infection.

Finally, we identified KIF4 as a critical host factor necessary for effective HBV infection. KIF4 controls the levels of surface NTCP by anterograde transport of NTCP to the cell surface, which is needed for NTCP to function as a receptor for HBV and/or HDV

entry. NTCP is the major transporter of conjugated bile salts from the plasma compartment into the hepatocyte. Although the loss of surface NTCP expression in a patient with the homozygous SLC10A1 gene containing a R252H point mutation showed higher levels of bile salts in the plasma, however, it did not show any evidence of cholestatic jaundice, pruritis, or liver dysfunction. Importantly, the presence of secondary bile salts in his circulation suggested residual enterohepatic cycling of bile salts (29). Furthermore, in NTCP knockout mice, some showed a reduced body weight, however, most animals showed no signs of cholestasis, inflammation, or hepatocellular damage (30). While further in-vivo data are still required to assess efficiency and safety of NTCP targeting drugs, the available data suggest its possible use for the prophylactic treatment against HBV infection. HBIG is used to inhibit HBV vertical transmission (31). Furthermore, extended therapy with HBIG in conjunction with a nucleos(t)ide analog is necessary following liver transplantation (LT) to reduce the HBV recurrence rate to less than 10% in 1-2 years post-transplantation (32). Bexarotene, which inhibits HBV cell entry, might be utilized as an alternative to HBIG. Because HBV entry inhibition reduces the intrahepatic cccDNA pool (33), entry inhibitors are expected to be useful in preventing de novo infection in clinical settings such as vertical transmission and HBV recurrence post-LT. These data strongly suggest that Bexarotene and its derivatives would be studied

366 further for the development of a new class of anti-HBV agents.

367

368 ## Materials and Methods:

369 **Cell culture**

370 HepG2, HepG2-hNTCP-C4, HepAD38.7-Tet, primary human hepatocytes
371 (Phoenixbio; PXB cells), and HEK 293FT cells were cultured as previously described
372 (16). For maintenance, HepG2-hNTCP cells were cultured in 400 µg/mL G418 (34),
373 while HepAD38.7-Tet cells were cultured in 0.4 µg/mL tetracycline that is withdrawn
374 from the medium upon induction of HBV replication (35).

375 **Reagents and compounds**

376 Sulfo-NHS-LC-Biotin (A39257) was purchased from Invitrogen. Myrcludex-B was
377 provided by Dr. Stephan Urban, at the University Hospital Heidelberg. Bexarotene
378 (SML0282), ATRA (R2625), Tamibarotene (T3205), Alitretinoin (R4643), Entecavir, and
379 DMSO were all purchased from Sigma-Aldrich.

380 **Human genome siRNA library screening**

381 siRNA screening was performed as reported previously (36). Briefly, HBV host factors
382 were screened using the Silencer Select™ Human Druggable Genome siRNA Library V4
383 transfection in HepG2-hNTCP cells. siRNAs were arrayed in 96-well-plates, and negative

384 control siRNA and si-NTCP were added to control the data obtained from each of the 96-
385 well-plates. siRNAs with different sequences targeting the same genes were distributed
386 across 3 plates (A, B, and C). Plates utilized in this screening are described elsewhere
387 (16).

388 **HBV/NL preparation and infection assay**

389 Reporter HBV/NL particles carrying recombinant HBV virus encoding NL gene were
390 collected from the supernatant of HepG2 cells transfected by pUC1.2xHBV/NL plasmid
391 expressing HBV genome (genotype C) in which the core region is substituted with NL-
392 encoding gene, and pUC1.2xHBV-D helper plasmid carrying packaging-deficient HBV
393 genome as described previously (22, 36). HBV/NL infection was performed 2 days after
394 siRNA transfection. At 8 dpi, the cells were lysed, and the Nano-Luc reading was
395 measured using the Nano-Glo® Luciferase Assay System (Promega, N1150), according
396 to the manufacturer's instructions.

397 **RNA and DNA transfection**

398 The cells were reverse transfected with siRNAs using Lipofectamine RNAiMAX
399 (Invitrogen) according to the manufacturer's guidelines. Forward siRNA transfection in
400 PXB cells was also performed using Lipofectamine RNAiMAX. Transfection with
401 plasmid DNA was performed using the Lipofectamine 3000 (for HepG2 and HepG2-

hNTCP) or Lipofectamine 2000 (For 293FT cells), according to the manufacturer's protocol. siRNA/Plasmid DNA co-transfection in HepG2 or HepG2-hNTCP was implemented with Lipofectamine 2000.

Plasmids and siRNAs:

N-terminal HaloTag KIF4 expressing plasmid (pFN21ASDB3041) was purchased from Promega. The N-terminal Myc-tagged KIF4 (both wild type and ATPase-null motor inactive mutant) cloned in the pIRESpuro3 expression vector was kindly provided by Dr. Toru Hirota at Cancer Institute of the Japanese Foundation for Cancer Research (JFCR). Myc-tagged KIF4 motor inactive mutant was created by substituting 94 aa lysine in the ATP-binding Walker A consensus site to alanine (37). HA-tagged NTCP was kindly provided by Dr. Hiroyuki Miyoshi at RIKEN BioResource Research Center, Japan (38). pUC1.2xHBV/NL and pUC1.2xHBV-D plasmids were kindly supplied by Dr. Kunitada Shimotohno at National Center for Global Health and Medicine, Japan. pSVLD3 plasmid was kindly provided by Dr. John Taylor at the Fox Chase Cancer Center, USA. Silencer Select™ si-KIF4 (si-1, s24406; si-2, s24408), si-NTCP (s224646), control siRNA (#1), and customized si-KIF4 3′ UTR targeting endogenous KIF4 mRNA 3`-UTR region (5′-GGAAUGAGGUUGUGAUCUUTT-3′) were purchased from Thermo Fisher Scientific.

HBV infection assay

HBV (genotype D) particles were concentrated from the culture supernatant of HepAD38.7 Tet cells as described elsewhere (34). HepG2-hNTCP and primary human hepatocytes (PXB) were inoculated with HBV at 6000 and 1000 genome equivalent (GEq)/cell, respectively, as described previously (16).

HBV preS1 binding assay

HBV preS1 peptide spanning 2–48 amino acids of the preS1 region with N-terminal myristoylation, and C-terminal 6-carboxytetramethylrhodamine (TAMRA) conjugation (preS1 probe) was synthesized by Scrum, Inc. EZ-Link™. The attachment of HBV preS1 peptide to the HepG2-hNTCP cell surface was performed and analyzed as described previously (38).

HDV infection assay

HDV used in the infection assay was derived from the culture supernatant of Huh7 cells co-transfected with pSVLD3 and pT7HB2.7 as previously reported (39, 40). HepG2-hNTCP and primary human hepatocytes (PXB) were infected with HDV at 40–50 GEq/cell as described previously (41).

Dual-luciferase reporter assay

HepG2 cells were co-transfected with effector plasmid (Mock or KIF4), the *Firefly* luciferase reporter vectors, and the *Renilla* luciferase plasmid pRL-TK (Promega) as an

438 internal control. The reporter plasmids carrying the entire core promoter (nucleotide [nt]
439 900–1817), preS1 promoter (nt 2707–2847), preS2/S promoter (nt 2937–3204), or
440 Enh1/X promoter (nt 950–1373) upstream of the *Firefly* luciferase gene, has been
441 reported previously (42). At 2 days after transfection, the cells were lysed and the
442 luciferase activities were measured using the GloMax® 96 Microplate Luminometer
443 (Promega, GMJ96).

444 **HBV replication assay**

445 In the absence of tetracycline, HepAD38.7-Tet cells were reverse transfected with si-
446 control or si-KIF4 or treated with 10 μM entecavir as a positive control. At 4 days post-
447 transfection, the cells were lysed and the intracellular HBV DNA was extracted and
448 quantified by real-time PCR (35).

449 **Indirect immunofluorescence assay**

450 Immunofluorescence assay was basically performed as described previously (43).
451 primary antibodies used in the study included rabbit anti- HBc (Neomarkers, RB-1413-
452 A), anti-HDAg, anti-NTCP (Sigma, HPA042727), mouse anti-c-Myc (Santa Cruz, sc-40),
453 and anti-α-tubulin (Sigma, T5168). Alexa Flour555-, Alexa Flour488-, or Alexa
454 Flour647-conjugated secondary antibodies (Invitrogen) were utilized together with DAPI
455 to visualize the nucleus. For Halo tag, live cells were treated with cell-permeant Halotag

TMR ligand (Promega, G8251) before paraformaldehyde fixation. Microscopic examination of the infected cells or preS1 binding was performed by fluorescence microscopy (KEYENCE, BZ-X710); the observation of the subcellular localization was performed using a high-resolution confocal microscope (Leica, TCS 159 SP8) as described previously (43).

Immunoblot assay

Immunoblotting and protein detection were essentially performed as previously described (44). Protein detection was performed using the following primary antibodies; mouse monoclonal E-cadherin antibody (Santa-Cruz, sc-8426), anti-GAPDH (Abcam, ab9484), anti-Myc (Santa Cruz, sc-40), anti-β-actin (Sigma-Aldrich, A5441), anti-FOXM1 (Santa Cruz, sc-271746); and rabbit polyclonal anti-KIF4A (Invitrogen, PA5-30492), anti-NTCP (Sigma, HPA042727), anti-HA (Sigma, H6908). For immunoblotting of free or tagged NTCP, the sample was treated with 250-U Peptide-N-Glycosidase F (PNGase F) to digest N-linked oligosaccharides from glycoproteins before loading to SDS-PAGE (43).

Cell surface biotinylation and extraction of surface proteins

Cell surface biotinylation was performed to separate the surface proteins with streptavidin beads. The cells were washed with PBS and then incubated with 0.5 mg/mL

474 EZ-Link™ Sulfo-NHS-LC-Biotin for 30 min at 4°C to biotinylate the cell surface
475 proteins. After quenching with PBS containing 0.1% BSA and washing with PBS thrice
476 to remove free inactive biotin, the cells were lysed in lysis buffer (150 mM NaCl, 50 mM
477 Tris-HCL PH 7.4, 5 mM EDTA, 1% NP40) containing 1x protease inhibitor (Roche) for
478 15 min at 4°C. The cell lysate was centrifuged, and the supernatant was harvested and
479 added to pre-washed streptavidin agarose (SA) beads and incubated for 2 h at 4°C (Pull-
480 down step). Finally, the SA beads were washed with lysis buffer, and the adsorbed
481 proteins were eluted in the sample buffer and subjected to immunoblot assay as described
482 earlier. The surface adhesion protein E-cadherin (CDH-1) was used as a loading control
483 for biotinylated surface fraction, as reported elsewhere (45).

484 **Purification of cytoplasmic fraction**

485 The cells were washed with cold PBS, lysed, and subjected to cell fractionation; the
486 cytosolic fraction was isolated from the whole cell lysate using the Minute ™ Plasma
487 Membrane Protein Isolation and Cell Fractionation Kit (Invent Biotechnologies)
488 according to the manufacturer's protocol (46).

489 **Co-Immunoprecipitation (Co-IP) assay**

490 293FT cells were transfected with HA-tagged NTCP and Myc-tagged KIF4 expression
491 plasmids at a 1:1 ratio for the assessment of the possible physical interaction between

492 NTCP and KIF4. At 72 h after transfection, the cells were lysed and subjected to
493 immunoprecipitation with the mouse monoclonal anti-Myc (Santa-Cruz) antibody or
494 mouse normal IgG as a negative control. Cell lysis and Co-IP were conducted using the
495 Pierce™ Co-IP Kit (Thermo Fisher Scientific, 26149) according to the manufacturer's
496 instructions.

497 **DNA and RNA extraction**

498 Intracellular HBV DNA was extracted from the cells using the QIAamp Mini Kit
499 (QIAGEN), and the extracellular HBV DNA was recovered from the supernatant using
500 the SideStep Lysis and Stabilization Buffer (Agilent Technologies, 400900), while RNA
501 extraction was performed using the NucleoSpin® RNA XS Kit (MACHEREY-NAGEL)
502 according to the manufacturer's protocols.

503 **Southern blot analysis**

504 Southern blotting was performed to detect intracellular HBV DNAs as described
505 previously (43).

506 **qPCR and RT-qPCR**

507 Real-time PCR (for the detection of total HBV DNA) and reverse transcription real-
508 time PCR (for the measurement of HDV RNA) were essentially performed as previously
509 described (41, 47) using the primer-probe sets; 5′-AAGGTAGGAGCTGGAGCATTCG-

3′, 5′-AGGCGGATTTGCTGGCAAAG-3′, 5′-FAM-AGCCCTCAGGCTCAGGGCATAC-TAMRA-3′ for HBV DNA, and 5′-GGACCCCTTCAGCGAACA-3′, 5′-CCTAGCATCTCCTCCTATCGCTAT-3′, 5′-FAM-AGGCGCTTCGAGCGGTAGGAGTAAGA-TAMRA-3′ for HDV RNA. qPCR for Intracellular HBV DNA was performed by the $2^{(-\Delta\Delta CT)}$ method using chromosomal GAPDH DNA sequence (via primer-probe set Hs04420697_g1; Applied Biosystems) as an internal normalization control. Isolated RNA was reverse-transcribed using the High-Capacity cDNA Reverse Transcription Kit (Thermo Fisher Scientific), and the relative levels of the KIF4 mRNA were determined using the TaqMan Gene Expression Assay with the primer-probe set Hs00602211_g1 (Applied Biosystems), while the ACTB expression (primer-probe set 748 Hs99999903_m1) was included as an internal control for normalization (36).

ELISA

Cell supernatants were harvested and ELISA quantification of the secreted HBs was performed as described previously (47). The half-maximal inhibitory concentration (IC_{50}) value for Bexarotene was calculated as described previously (38).

Cell viability assay

Cell viability was evaluated using the Cell Proliferation Kit II (XTT) according to the

manufacturer's guidelines (43).

Database

Transcriptional profiling of patients with chronic HBV (NCBI Gene Expression Omnibus [GEO] accession number GSE83148) was identified in the GEO public database. The expression data for KIF4 were extracted by GEO2R.

Statistical analysis

Unless mentioned otherwise, the experiments were performed in triplicates, and the means of data from three independent experiments were calculated and presented in mean ± SD. Statistical significance was determined using Two-tailed unpaired student's *t*-tests (*, $P < 0.05$; **, $P < 0.01$; ***, $P < 0.001$; NS, not significant). For the KIF4 expression level in chronic HBV (NCBI [GEO] accession number GSE83148), statistical significance was evaluated by GEO2R to calculate the adjusted *P* value.

Acknowledgments

S.A.G was the recipient of the Egyptian Japanese Education Partnership-3 (EJEP-3) PhD scholarship provided by the Ministry of Higher Education of Egypt. This study was supported by a Grant-In-Aid for Scientific Research (19K07586), and grants from the Research Program on Hepatitis from the Japan Agency for Medical Research and Development (AMED; 21fk0310104j0905, 21fk0310109j0405, 21fk0310103j0305, and

546 20fk0310109h0004). We gratefully acknowledge Dr. Stephan Urban at University
547 Hospital Heidelberg for providing Myrcludex-B; Dr. Toru Hirota at JFCR, Japan for
548 providing Myc-tagged KIF4 (both Wild Type and motor inactive mutant); Dr. John Taylor
549 at the Fox Chase Cancer Center, the USA for providing pSVLD3 plasmid; and Dr.
550 Hiroyuki Miyoshi at RIKEN, Japan, for providing HA-tagged NTCP.

551

552 ## Figure Legends

553 **FIG. 1**

554 **KIF4 is a proviral host factor required for HBV infection and its expression is**
555 **enhanced in chronic hepatitis B patients.**

556 **(A)** A schematic representation of the experimental HBV/NL infection schedule in
557 HepG2-hNTCP used for siRNA library screening. **(B)** HepG2-hNTCP cells were
558 transfected with control, NTCP, or host gene targeting siRNAs from the Silencer Select
559 Human Druggable Genome siRNA Library V4 (Thermo Fisher Scientific, 4397922); host
560 genes siRNA plates were screened as described in the *Material* and *Methods* section. After
561 2 days of transfection, the cells were inoculated with the HBV/NL reporter virus. At 8 dpi,
562 the luciferase assays were performed, and the NL activity was measured and presented as
563 a percentage relative to control siRNA transfected cells. Of the 2,200 host genes, only 14
564 genes showed an average of ≥70% reduction of the NL activity upon silencing with a

565 minimum of two independent siRNAs. **(C)** The KIF4 mRNA levels in the liver tissues of
566 patients with chronic HBV infection (n = 122) and healthy subjects (n = 6) (GEO
567 accession number GSE83148). **(D)** HepG2-hNTCP cells were transfected with si-control,
568 si-NTCP, or siRNAs against KIF4 (si-1, and si-2) for 2 days and then inoculated with the
569 HBV/NL reporter virus. At 8 dpi, the cells were lysed, and the luciferase assays were
570 performed, and the NL activity was measured, normalized to cell viability, and plotted as
571 fold changes, relative to control siRNA transfected cells. **(E)** HepG2-hNTCP cells were
572 transfected with control siRNA or siRNAs against KIF4 (si-1 and si-2); the total protein
573 was extracted after 3 days. The expression of endogenous KIF4 (*upper panel*) and β-actin
574 (loading control) (*lower panel*) was analyzed by immunoblotting with the respective
575 antibodies. Statistical significance was determined using Student's *t*-test (***, $P < 0.001$).
576 For panel (C), statistical significance was evaluated by GEO2R.

577 **FIG 2**

578 **Decreased KIF4 expression suppressed HBV infection in HepG2-hNTCP and**
579 **primary human hepatocytes (PHH).**

580 **(A)** Schematic diagram depicting the scheme for siRNA transfection and subsequent HBV
581 infection in HepG2-hNTCP; HepG2-hNTCP cells were transfected with si-control, si-
582 NTCP, or si-KIF4 (si-1) for 72 h and then inoculated with HBV at 6,000 GEq/cell in the

583 presence of 4% PEG8000 for 16 h. After free HBV were washed out, the cells were
584 cultured for an additional 12 days, followed by the detection of different HBV
585 markers. Black and dashed boxes indicate the interval for treatment and without
586 treatment, respectively. **(B)** HBsAg secreted into the culture supernatant was collected at
587 10 dpi, quantified by ELISA, and presented as fold changes, relative to the values of
588 control siRNA transfected cells. **(C)** Intracellular HBV DNA and **(D)** HBc protein in the
589 cells were detected at 13 dpi by Southern blot analysis and immunofluorescence,
590 respectively. Red and blue signals in panel **(D)** depict the staining of HBc protein and
591 nucleus, respectively. **(E)** Cell viability was also examined by the XTT assay. **(F)**
592 Schematic diagram showing the scheme for siRNA transfection and the subsequent HBV
593 infection in primary human hepatocytes (PXB); primary human hepatocytes were twice
594 transfected with si-control, si-NTCP, or si-KIF4 (si-1) for consecutive 72 h and 48 h,
595 followed by HBV inoculation at 1,000 GEq/cell in the presence of 4% PEG8000 for 16
596 h. After being washed, the cells were cultured for an additional 15 days. **(G)** HBsAg and
597 **(H)** Extracellular HBV-DNA secreted into the culture supernatant were quantified by
598 ELISA and real-time PCR, respectively, and the data were presented as fold changes,
599 relative to the values of control siRNA-transfected cells. In all infection assays including
600 siRNA transfection, control siRNA and NTCP-targeting siRNA were used as negative and

positive controls, respectively. (**I**) Primary human hepatocytes were twice transfected with siRNAs (as shown in Fig. 2 F); the total protein was extracted and KIF4 (*upper panel*) and β-actin (loading control) (*lower panel*) expression were analyzed by immunoblotting with the respective antibodies. All assays were performed in triplicate and included 3 independent experiments. Standard deviations are also shown as error bars. Statistical significance was determined using Student's *t*-test (**, $P < 0.01$; ***, $P < 0.001$; NS, not significant).

FIG.3

KIF4 knockdown blocks HBV entry and HDV infection into host cells.

(A) HepG2-hNTCP were transfected with si-control, si-NTCP, or si-KIF4 (si-1) for 72 h and then incubated with 40 nM C-terminally TAMRA labeled and N-terminally myristoylated preS1 peptide (preS1 probe) for 30 min at 37°C (*left panel*); Red and blue signals indicate the preS1 probe and the nucleus, respectively. The fluorescence intensities are shown in the graph (*right panel*). **(B)** HepG2 cells were transfected with a KIF4 expression vector or empty vector (control) together with plasmid vector carrying HBV promoters (Core, X, preS1, or preS2/S) upstream of the *Firefly* luciferase gene and the pRL-TK control plasmid encoding *Renilla* luciferase. At 2 days post-transfection, the cells were lysed and the dual-luciferase activities were measured; the *Firefly* luciferase

values were normalized to those of *Renilla* luciferase readings, and the resulting relative luminescence units obtained from KIF4 transfected cells were presented as fold changes compared to the levels detected in the control transfected cells. **(C)** HepAD38.7-Tet cells were transfected with si-control or si-KIF4 (si-1) or treated with 10-μM entecavir as a positive control in the absence of tetracycline to induce HBV replication; At 4 days post-transfection, the cells were lysed and the intracellular HBV DNA was extracted and quantified by real-time PCR. **(D)** HepG2-hNTCP were transfected with siRNAs (as indicated in **Fig. 3A**), and then inoculated with HDV virions at 50 GEq/cell in the presence of 5% PEG8000 for 16 h; the cells were then washed out to remove the free virus particles and cultured for an additional 6 days, followed by detection of HDAg by IF (*left panel*); Red and blue signals indicate HDAg and nuclear staining, respectively. The fluorescence intensities are shown in the graph (*right panel*). All assays were performed in triplicate and included three independent experiments. The data were pooled to assess the statistical significance. Data are presented as mean ± SD. **, $P < 0.01$; ***, $P < 0.001$; NS, not significant.

FIG 4

KIF4 regulates the surface NTCP expression.

(A) HepG2-hNTCP were transfected with either si-control or si-KIF4 (si-1) and incubated

for 72 h; the cells were then lysed and the expressions of total NTCP (*upper panel*), KIF4 (*middle panel*), and β-actin (loading control) (*lower panel*) were examined in the whole protein lysate by Western blotting. **(B)** HepG2-hNTCP were transfected with si-RNAs (as in **Fig. 4A**) and incubated for 72 h; the cells were then fixed with 4% paraformaldehyde, permeabilized with 0.3% Triton X-100, and stained with NTCP antibody and visualized with confocal microscopy. Green and blue signals depict the staining of NTCP (both surface and cytoplasmic), and nuclei, respectively. **(C)** HepG2-hNTCP were transfected with si-RNAs (as in **Fig. 4A**); at 3 days post-transfection, the cells were surface biotinylated or PBS treated at 4°C for 30 min before cell lysis. After centrifugation and the removal of cell debris, the cell lysates were collected and an aliquot (1/10 volume) was used for the detection of NTCP protein (*Input; upper panel*) and β-actin (loading control) (*Input; lower panels*) by immunoblotting. The remaining cell lysates (9/10 of the original volume) were subjected to pull-down via incubation with pre-washed SA beads for 2 h at 4°C; after washing, the biotinylated surface proteins were eluted and subjected to western blotting in order to detect the surface NTCP and CDH-1 (loading control for surface fraction) (*Surface; upper*, and *lower panels*) with the respective antibodies. **(D)** After transfection with siRNAs (as shown in **Fig. 4A**), HepG2-hNTCP cells were lysed and the cytoplasmic fraction was isolated, harvested using the Minute ™ Plasma

Membrane Protein Isolation and the Cell Fractionation Kit and then subjected to immunoblotting in order to detect the cytoplasmic NTCP (*upper panel*) and GAPDH (loading control for cytoplasmic fraction) (*lower panel*). **(E)** The intensities of both the surface (normalized to CDH-1) and cytoplasmic (normalized to GAPDH) NTCP bands were quantified by ImageJ software and presented as fold changes relative to the control siRNA transfected cells.

FIG 5

KIF4 motor activity is required for the surface NTCP expression.

(A) A schematic diagram illustrating human KIF4 domains and the key regions are presented at the top of the figure. Two sequence alignments show ATP-binding Walker A consensus site in the KIF4 motor domain with lysine 94 (Wild type, *upper sequence*) was mutated to alanine (ATPase-null motor dead mutant, *lower sequence*). **(B)** HepG2 cells were transfected with si-KIF4 3′ UTR (targeting endogenous KIF4 mRNA 3` UTR region) along with HA-NTCP, and Myc-KIF4 (WT or ATPase-null) plasmid vectors for 72 h; the cells were then surface biotinylated or PBS treated at 4°C for 30 min before cell lysis. After centrifugation and the removal of cell debris, cell lysates were collected and an aliquot (1/10 volume) was used for the detection of HA-NTCP (*input; upper panel*), Myc-KIF4 (*Input; middle panel*), and β-actin (loading control) (*Input; lower panel*) by

673 immunoblotting. The remaining cell lysates (9/10 of the original volume) were subjected
674 to pull-down via incubation with pre-washed SA beads for 2 h at 4°C; after being washed,
675 the biotinylated surface proteins were eluted and subjected to western blotting in order to
676 detect surface HA-NTCP (*Surface; upper panel*) and CDH-1 (loading control for surface
677 fraction) (*Surface; lower panel*) with the respective antibodies. **(C)** HepG2-hNTCP were
678 transfected with si-KIF4 3′ UTR and Myc-KIF4 WT (*upper panel*) or motor dead mutant
679 (*lower panel*) plasmid vectors; at 3 days post-transfection, the cells were fixed,
680 permeabilized, stained with the indicated antibodies, and visualized by confocal
681 microscopy. Green, red, and blue signals represent the staining of NTCP, Myc-KIF4, and
682 nuclei, respectively. The arrow heads show NTCP localization in the WT or ATPase-null
683 KIF4 transfected cells. **(D)** HepG2-hNTCP were transfected with si-control or si-KIF4 3′
684 UTR for 48 h; the cells were then lysed and the total RNA content was extracted and the
685 KIF4 expression levels were quantified by RT-qPCR and normalized to the expression of
686 ACTB; or **(E)** the cell viability was examined using XTT assay. Data are presented as
687 fold changes, relative to those of the control siRNA-transfected cells. All assays were
688 performed in triplicate and data from 3 independent experiments were included. The data
689 were pooled to assess the statistical significance. Data are presented as mean ± SD. ***,
690 $P < 0.001$; NS, not significant.

FIG 6

Interaction of KIF4 and NTCP over microtubule filaments.

(A) HepG2-hNTCP were transfected with a Halo-tagged KIF4 expression vector or empty vector (control). At 48 h post-transfection, the cells were incubated with Halo-tag TMR ligand for 15 min at 37°C; after being washed, cells were fixed, and permeabilized. The cells were stained with antibodies against NTCP and α-tubulin, as indicated in the *Materials* and *Methods* section and examined by confocal microscopy. Blue, green, red, and purple signals indicate nuclear, NTCP, KIF4, and microtubular (α-tubulin) staining, respectively (*upper panel*). White arrows indicate colocalization signals of NTCP and KIF4 over microtubule filaments. The middle panel shows two irrelevant lines crossing different regions of interest within the overlay pattern and represented by their corresponding colocalization signal intensity charts (*lower panel*). **(B)** HEK293-FT cells were co-transfected with HA-NTCP, and Myc-KIF4 plasmid vectors (at a ratio of 1:1). At 3 days post-transfection, the cells were lysed and an aliquot of the cell lysate (1/10 volume) was used for the detection of Myc-KIF4 (*Input; upper panel*), HA-NTCP (*Input; middle panel*), and β-actin (loading control) (*Input; lower panel*) by immunoblotting. The remaining cell lysates (9/10 of the original volume) were subjected to co-IP using either isotype control antibody or anti-Myc IgG to pull down Myc-KIF4. Following IP, each

sample was analyzed by immunoblotting for Myc-KIF4 (*IP; upper panel*) and co-immunoprecipitated HA-NTCP (*IP; lower panel*). All assays were performed in triplicate and data from 3 independent experiments were included.

FIG 7

RXR agonists suppressed KIF4 mediated surface NTCP transport, blocked HBV entry, and inhibited HBV/NL infection in HepG2-hNTCP. (A) HepG2-hNTCP pretreated with DMSO, 10 μM of the indicated compounds (Bexarotene, ATRA, Tamibarotene) (*upper panel*), or alitretinoin (10 μM) (*lower panel*) for 72 h were incubated with TAMRA-labeled preS1 peptide (preS1 probe) for 30 min at 37°C and then examined by fluorescence microscopy. DMSO-treated cells were incubated with a preS1 probe either in the absence (negative control) or presence (positive control) of 100 nM Myrcludex B (Myr-B); Red and blue signals indicate preS1 probe and the nucleus, respectively. (B) HepG2-hNTCP were treated with DMSO or 10 μM Bexarotene for 72 h, the cells were then surface biotinylated or PBS treated at 4°C for 30 min prior to cell lysis, the cell lysates were collected and an aliquot (1/10 volume) was used for detection of NTCP protein (input) (*Input; upper panel)* and β-actin (loading control) by immunoblotting (*Input; lower panel*). The remaining cell lysates (9/10 of the original volume) were subjected to pull-down via incubation with pre-washed SA beads for 2 h at

4°C; after washing, the biotinylated surface proteins were eluted and subjected to western blotting to detect the surface NTCP (*Surface*; *upper* panel) and CDH-1 (loading control for surface fraction) (*Surface*, *lower panel*) with the respective antibodies. **(C)** HepG2-hNTCP cells treated with DMSO or 10 μM Bexarotene for 72 h were lysed and total cell lysates were subjected to immunoblotting to detect the protein expression levels of KIF4 (*upper panel*), FOXM1 (*middle panel*), and β-actin (loading control) (*lower panel*) with their corresponding antibodies. **(D)** HepG2-hNTCP were pretreated with DMSO or 10 μM Bexarotene for 72 h; then DMSO and Bexarotene were withdrawn from the culture medium 3 h before HBV/NL inoculation, and the cells were inoculated with the HBV/NL reporter virus for 16 h. DMSO-pretreated cells were concomitantly treated with or without 100 nM Myr-B during HBV/NL inoculation. At 8 dpi, the cells were lysed, luciferase assays were performed, and NL activity was measured, and then plotted as fold changes, relative to the values of control DMSO-pretreated cells. **(E)** HepG2-hNTCP were exposed to DMSO or different concentrations of Bexarotene (1 μM, 10 μM, and 20 μM) for 72 h; cell viability was then evaluated by XTT assay. All assays were performed in triplicate and data from 3 independent experiments were included. The data were pooled to assess the statistical significance. Data are presented as mean ± SD. ***, $P < 0.001$.

FIG 8

745 **Bexarotene pretreatment significantly suppressed HBV and HDV infections in**
746 **primary human hepatocytes (PHH). (A)** A schematic representation showing the
747 protocol used for Bexarotene treatment and subsequent HBV infection in PHH; PHH
748 were pretreated with DMSO or different concentrations of Bexarotene (1 μM, 10 μM, 20
749 μM, and 50 μM) for 72 h, DMSO and Bexarotene were withdrawn from the culture
750 medium 3 h before HBV infection, and the cells were inoculated with HBV particles at
751 1,000 GEq/cell in the presence of 4% PEG8000 for 16 h. DMSO-pretreated cells were
752 concomitantly treated with or without 100 nM Myr-B during HBV inoculation. After
753 being washed, the cells were cultured for an additional 15 days. **(B)** HBsAg secreted into
754 the culture supernatant was quantified by ELISA, and the data were presented as fold
755 changes relative to the values of control DMSO-pretreated cells. **(C)** Cell viability were
756 measured by the XTT assay. (**D**) A schematic diagram showing HBV infection protocol;
757 PHH were treated with 15 μM Bexarotene at different time schedule (pre, co, post, and
758 whole) as shown in the figure. The cells were inoculated with HBV at 1,000 GEq per cell
759 in the presence of 4% PEG8000 for 16 h. Bexarotene non-treated cells were
760 concomitantly incubated with or without 100 nM Myr-B during HBV inoculation. After
761 washing out the free virus particles, the cells were cultured for an additional 11 days. (**E**)
762 HBc protein in the cells was detected by immunofluorescence. Red and blue signals depict

763 the staining of HBc protein and nucleus (dapi), respectively and HBc fluorescence
764 intensities are shown in Panel (**F**). **(G)** PHH pretreated with DMSO or Bexarotene (50
765 μM) for 72 h were inoculated with the HDV at 40 GEq/cell in the presence of 5%
766 PEG8000 for 16 h. DMSO-pretreated cells were concomitantly treated with or without
767 100 nM Myr-B during HDV inoculation. After washing out the free virus particles, the
768 cells were cultured for an additional 6 days and then lysed; RNA was then extracted and
769 HDV RNA was quantified by RT-qPCR. The data are presented as fold differences
770 relative to those of the control DMSO-pretreated cells. All assays were performed in
771 triplicate and data from 3 independent experiments were included. The data were pooled
772 to assess the statistical significance. For panels **(D and G)**, the assay was performed in
773 triplicate, and data from 2 independent experiments were pooled. Data are presented as
774 mean ± SD. *, $P < 0.05$; **, $P < 0.01$; ***, $P < 0.001$.
775
776 1. Nassal M. HBV cccDNA: viral persistence reservoir and key obstacle for a cure of chronic
777 hepatitis B. Gut. 2015;64(12):1972-84.
778 2. Sureau C, Negro F. The hepatitis delta virus: Replication and pathogenesis. J Hepatol.
779 2016;64(1 Suppl):S102-S16.
780 3. Yan H, Zhong G, Xu G, He W, Jing Z, Gao Z, et al. Sodium taurocholate cotransporting
781 polypeptide is a functional receptor for human hepatitis B and D virus. Elife. 2012;3.
782 4. Shi Y, Zheng M. Hepatitis B virus persistence and reactivation. BMJ. 2020;370:m2200.
783 5. Miki H, Setou M, Kaneshiro K, Hirokawa N. All kinesin superfamily protein, KIF, genes
784 in mouse and human. Proc Natl Acad Sci U S A. 2001;98(13):7004-11.
785 6. Skold HN, Komma DJ, Endow SA. Assembly pathway of the anastral Drosophila oocyte
786 meiosis I spindle. J Cell Sci. 2005;118(Pt 8):1745-55.

787 7. Endow SA, Kull FJ, Liu H. Kinesins at a glance. J Cell Sci. 2010;123(Pt 20):3420-4.
788 8. Powers J, Rose DJ, Saunders A, Dunkelbarger S, Strome S, Saxton WM. Loss of KLP-19
789 polar ejection force causes misorientation and missegregation of holocentric chromosomes. J Cell
790 Biol. 2004;166(7):991-1001.
791 9. Williams BC, Riedy MF, Williams EV, Gatti M, Goldberg ML. The Drosophila kinesin-
792 like protein KLP3A is a midbody component required for central spindle assembly and initiation
793 of cytokinesis. J Cell Biol. 1995;129(3):709-23.
794 10. Vernos I, Raats J, Hirano T, Heasman J, Karsenti E, Wylie C. Xklp1, a chromosomal
795 Xenopus kinesin-like protein essential for spindle organization and chromosome positioning. Cell.
796 1995;81(1):117-27.
797 11. Sheng L, Hao SL, Yang WX, Sun Y. The multiple functions of kinesin-4 family motor
798 protein KIF4 and its clinical potential. Gene. 2018;678:90-9.
799 12. Sabo Y, Walsh D, Barry DS, Tinaztepe S, de Los Santos K, Goff SP, et al. HIV-1 induces
800 the formation of stable microtubules to enhance early infection. Cell Host Microbe.
801 2013;14(5):535-46.
802 13. Zhou J, Scherer J, Yi J, Vallee RB. Role of kinesins in directed adenovirus transport and
803 cytoplasmic exploration. PLoS Pathog. 2018;14(5):e1007055.
804 14. Hu G, Yan Z, Zhang C, Cheng M, Yan Y, Wang Y, et al. FOXM1 promotes hepatocellular
805 carcinoma progression by regulating KIF4A expression. J Exp Clin Cancer Res. 2019;38(1):188.
806 15. Zhu CL, Cheng DZ, Liu F, Yan XH, Wu KL, Wang FB, et al. Hepatitis B virus
807 upregulates the expression of kinesin family member 4A. Mol Med Rep. 2015;12(3):3503-7.
808 16. Ibrahim MK, Abdelhafez TH, Takeuchi JS, Wakae K, Sugiyama M, Tsuge M, et al. MafF
809 Is an Antiviral Host Factor That Suppresses Transcription from Hepatitis B Virus Core Promoter.
810 J Virol. 2021;95(15):e0076721.
811 17. Zhou W, Ma Y, Zhang J, Hu J, Zhang M, Wang Y, et al. Predictive model for
812 inflammation grades of chronic hepatitis B: Large-scale analysis of clinical parameters and gene
813 expressions. Liver Int. 2017;37(11):1632-41.
814 18. Wu G, Chen PL. Structural requirements of chromokinesin Kif4A for its proper function
815 in mitosis. Biochem Biophys Res Commun. 2008;372(3):454-8.
816 19. Allweiss L, Volz T, Giersch K, Kah J, Raffa G, Petersen J, et al. Proliferation of primary
817 human hepatocytes and prevention of hepatitis B virus reinfection efficiently deplete nuclear
818 cccDNA in vivo. Gut. 2018;67(3):542-52.
819 20. Osei-Sarfo K, Gudas LJ. Retinoids induce antagonism between FOXO3A and FOXM1
820 transcription factors in human oral squamous cell carcinoma (OSCC) cells. PLoS One.
821 2019;14(4):e0215234.

822 21. Volz T, Allweiss L, Ben MM, Warlich M, Lohse AW, Pollok JM, et al. The entry inhibitor
823 Myrcludex-B efficiently blocks intrahepatic virus spreading in humanized mice previously infected
824 with hepatitis B virus. J Hepatol. 2013;58(5):861-7.
825 22. Nishitsuji H, Ujino S, Shimizu Y, Harada K, Zhang J, Sugiyama M, et al. Novel reporter
826 system to monitor early stages of the hepatitis B virus life cycle. Cancer Sci. 2015;106(11):1616-
827 24.
828 23. Hirokawa N, Noda Y, Tanaka Y, Niwa S. Kinesin superfamily motor proteins and
829 intracellular transport. Nature Reviews Molecular Cell Biology. 2009;10(10):682-96.
830 24. Heintz TG, Heller JP, Zhao R, Caceres A, Eva R, Fawcett JW. Kinesin KIF4A transports
831 integrin beta1 in developing axons of cortical neurons. Mol Cell Neurosci. 2014;63:60-71.
832 25. Tang Y, Winkler U, Freed EO, Torrey TA, Kim W, Li H, et al. Cellular motor protein
833 KIF-4 associates with retroviral Gag. J Virol. 1999;73(12):10508-13.
834 26. Cheng C, Michaels J, Scheinfeld N. Alitretinoin: a comprehensive review. Expert
835 Opinion on Investigational Drugs. 2008;17(3):437-43.
836 27. Jin Y, Huang J, Wang Q, He J, Teng Y, Jiang R, et al. RXR Negatively Regulates Ex Vivo
837 Expansion of Human Cord Blood Hematopoietic Stem and Progenitor Cells. Stem Cell Rev Rep.
838 2021;17(4):1456-64.
839 28. Song M, Sun Y, Tian J, He W, Xu G, Jing Z, et al. Silencing Retinoid X Receptor Alpha
840 Expression Enhances Early-Stage Hepatitis B Virus Infection In Cell Cultures. J Virol. 2018;92(8).
841 29. Vaz FM, Paulusma CC, Huidekoper H, de Ru M, Lim C, Koster J, et al. Sodium
842 taurocholate cotransporting polypeptide (SLC10A1) deficiency: conjugated hypercholanemia
843 without a clear clinical phenotype. Hepatology. 2015;61(1):260-7.
844 30. Slijepcevic D, Kaufman C, Wichers CG, Gilglioni EH, Lempp FA, Duijst S, et al.
845 Impaired uptake of conjugated bile acids and hepatitis b virus pres1-binding in na(+) -
846 taurocholate cotransporting polypeptide knockout mice. Hepatology. 2015;62(1):207-19.
847 31. Ma L, Alla NR, Li X, Mynbaev OA, Shi Z. Mother-to-child transmission of HBV: review
848 of current clinical management and prevention strategies. Rev Med Virol. 2014;24(6):396-406.
849 32. Samuel D, Muller R, Alexander G, Fassati L, Ducot B, Benhamou JP, et al. Liver
850 transplantation in European patients with the hepatitis B surface antigen. N Engl J Med.
851 1993;329(25):1842-7.
852 33. Tu T, Urban S. Virus entry and its inhibition to prevent and treat hepatitis B and
853 hepatitis D virus infections. Curr Opin Virol. 2018;30:68-79.
854 34. Iwamoto M, Watashi K, Tsukuda S, Aly HH, Fukasawa M, Fujimoto A, et al. Evaluation
855 and identification of hepatitis B virus entry inhibitors using HepG2 cells overexpressing a
856 membrane transporter NTCP. Biochem Biophys Res Commun. 2014;443(3):808-13.

857 35. Iwamoto M, Cai D, Sugiyama M, Suzuki R, Aizaki H, Ryo A, et al. Functional association
858 of cellular microtubules with viral capsid assembly supports efficient hepatitis B virus replication.
859 Sci Rep. 2017;7(1):10620.
860 36. Ibrahim MK, Abdelhafez TH, Takeuchi JS, Wakae K, Sugiyama M, Tsuge M, et al. MafF
861 is an antiviral host factor that suppresses transcription from Hepatitis B Virus core promoter. J
862 Virol. 2021.
863 37. Takahashi M, Wakai T, Hirota T. Condensin I-mediated mitotic chromosome assembly
864 requires association with chromokinesin KIF4A. Genes Dev. 2016;30(17):1931-6.
865 38. Fukano K, Tsukuda S, Oshima M, Suzuki R, Aizaki H, Ohki M, et al. Troglitazone
866 Impedes the Oligomerization of Sodium Taurocholate Cotransporting Polypeptide and Entry of
867 Hepatitis B Virus Into Hepatocytes. Front Microbiol. 2018;9:3257.
868 39. Kuo MY, Chao M, Taylor J. Initiation of replication of the human hepatitis delta virus
869 genome from cloned DNA: role of delta antigen. J Virol. 1989;63(5):1945-50.
870 40. Sureau C, Guerra B, Lee H. The middle hepatitis B virus envelope protein is not
871 necessary for infectivity of hepatitis delta virus. J Virol. 1994;68(6):4063-6.
872 41. Gudima S, Meier A, Dunbrack R, Taylor J, Bruss V. Two potentially important elements
873 of the hepatitis B virus large envelope protein are dispensable for the infectivity of hepatitis delta
874 virus. J Virol. 2007;81(8):4343-7.
875 42. Deng L, Gan X, Ito M, Chen M, Aly HH, Matsui C, et al. Peroxiredoxin 1, a Novel HBx-
876 Interacting Protein, Interacts with Exosome Component 5 and Negatively Regulates Hepatitis B
877 Virus (HBV) Propagation through Degradation of HBV RNA. J Virol. 2019;93(6).
878 43. Iwamoto M, Saso W, Sugiyama R, Ishii K, Ohki M, Nagamori S, et al. Epidermal growth
879 factor receptor is a host-entry cofactor triggering hepatitis B virus internalization. Proc Natl Acad
880 Sci U S A. 2019;116(17):8487-92.
881 44. Aly HH, Suzuki J, Watashi K, Chayama K, Hoshino S, Hijikata M, et al. RNA Exosome
882 Complex Regulates Stability of the Hepatitis B Virus X-mRNA Transcript in a Non-stop-mediated
883 (NSD) RNA Quality Control Mechanism. J Biol Chem. 2016;291(31):15958-74.
884 45. Londino JD, Gulick DL, Lear TB, Suber TL, Weathington NM, Masa LS, et al. Post-
885 translational modification of the interferon-gamma receptor alters its stability and signaling.
886 Biochem J. 2017;474(20):3543-57.
887 46. Mukhopadhyay S, Biancur DE, Parker SJ, Yamamoto K, Banh RS, Paulo JA, et al.
888 Autophagy is required for proper cysteine homeostasis in pancreatic cancer through regulation of
889 SLC7A11. Proc Natl Acad Sci U S A. 2021;118(6).
890 47. Watashi K, Liang G, Iwamoto M, Marusawa H, Uchida N, Daito T, et al. Interleukin-1
891 and tumor necrosis factor-alpha trigger restriction of hepatitis B virus infection via a cytidine
892 deaminase activation-induced cytidine deaminase (AID). J Biol Chem. 2013;288(44):31715-27.

893

Fig. 1

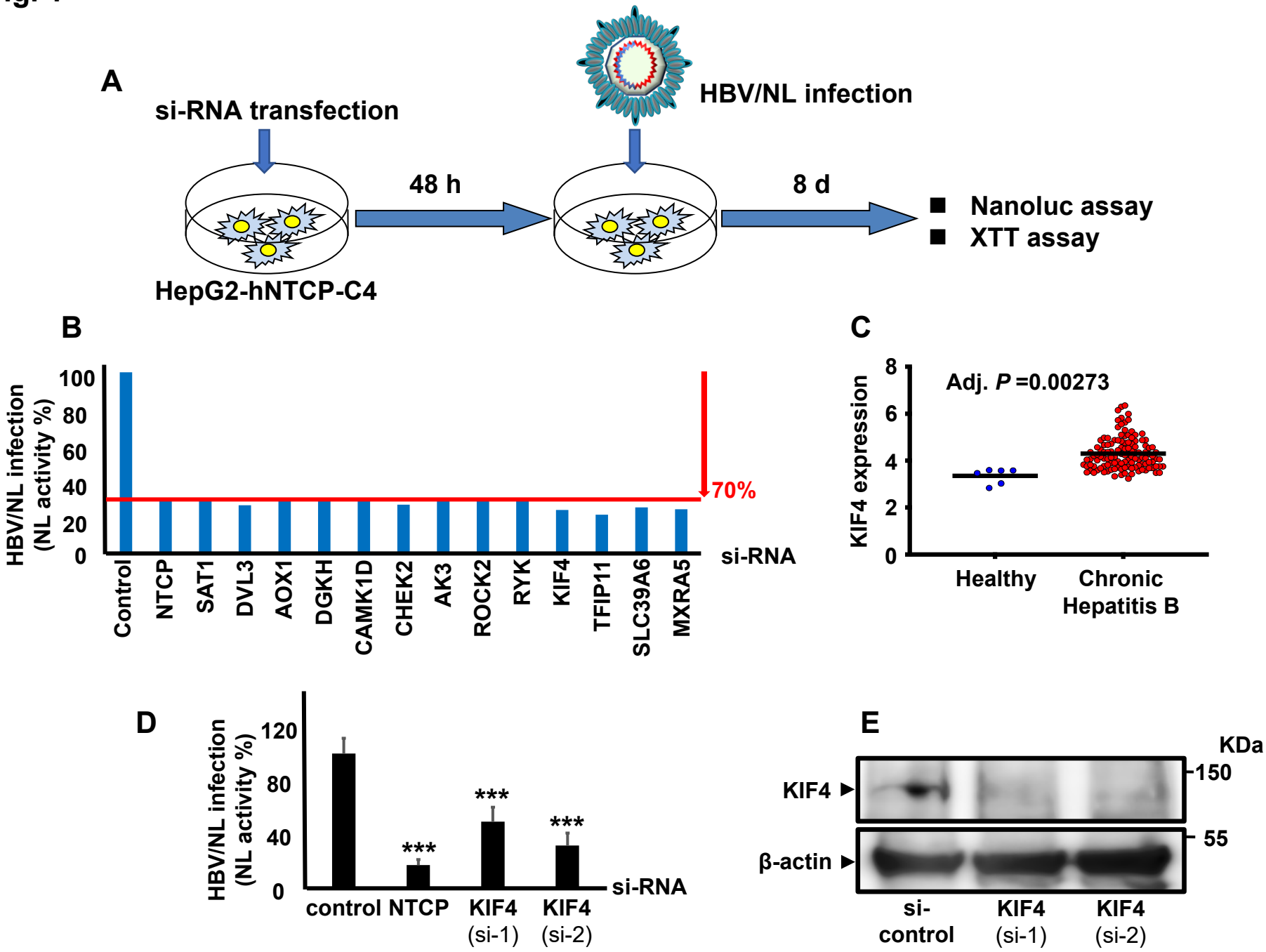
A
si-RNA transfection
HBV/NL infection
48 h
8 d
Nanoluc assay
XTT assay
HepG2-hNTCP-C4
B
HBV/NL infection (NL activity %)
100
80
60
40
20
0
70%
si-RNA
Control
NTCP
SAT1
DVL3
AOX1
DGKH
CAMK1D
CHEK2
AK3
ROCK2
RYK
KIF4
TFIP11
SLC39A6
MXRA5
C
KIF4 expression
8
6
4
2
0
Adj. P =0.00273
Healthy
Chronic Hepatitis B
D
HBV/NL infection (NL activity %)
120
80
40
0
***
***
***
si-RNA
control
NTCP
KIF4 (si-1)
KIF4 (si-2)
E
KDa
KIF4
β-actin
150
55
si-control
KIF4 (si-1)
KIF4 (si-2)

Fig. 2

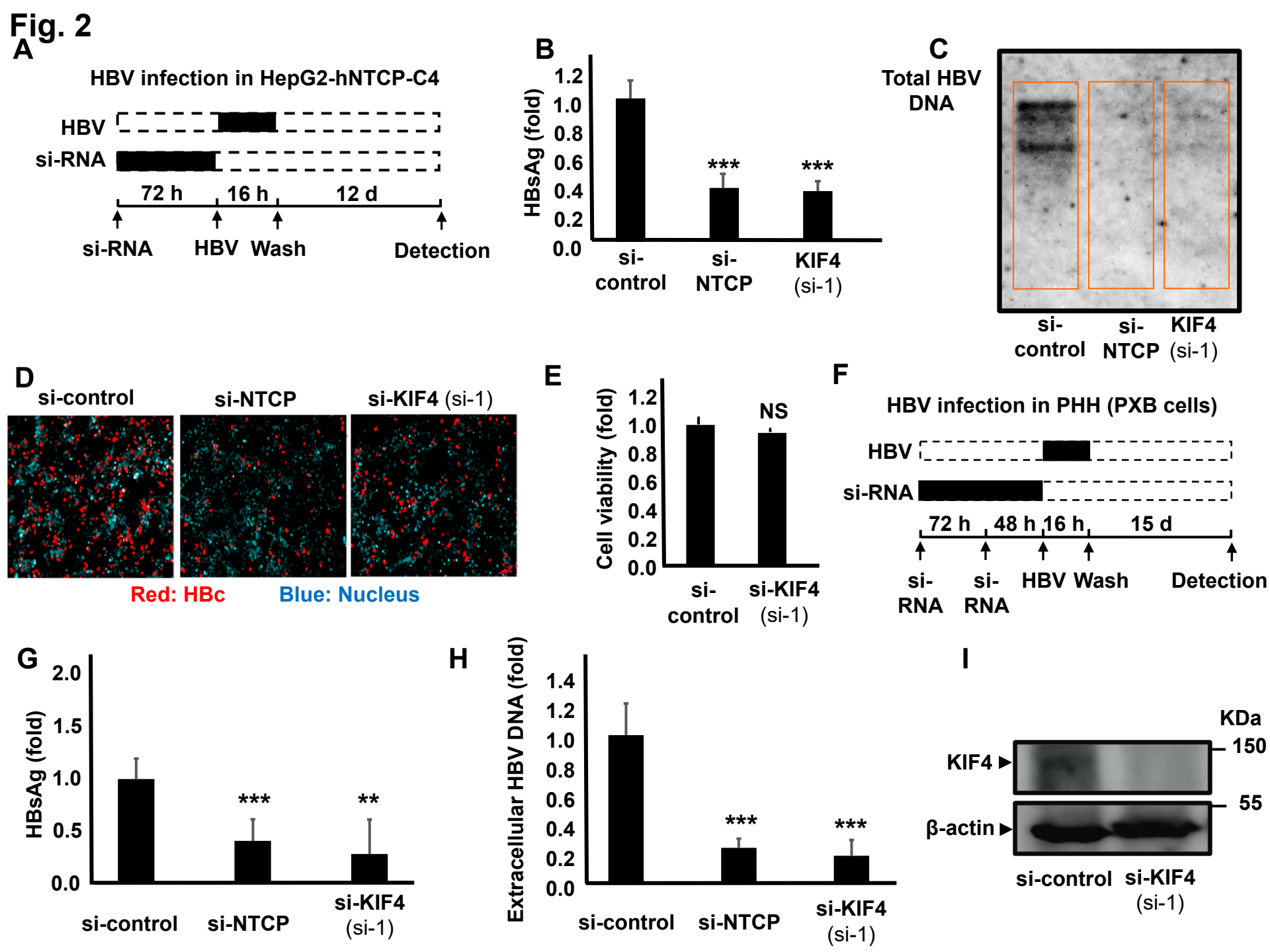
A
HBV infection in HepG2-hNTCP-C4
HBV
si-RNA
72 h
16 h
12 d
si-RNA
HBV
Wash
Detection
B
HBsAg (fold)
1.2
1.0
0.8
0.6
0.4
0.2
0.0
***
***
si-control
si-NTCP
KIF4 (si-1)
C
Total HBV DNA
si-control
si-NTCP
KIF4 (si-1)
D
si-control
si-NTCP
si-KIF4 (si-1)
Red: HBc
Blue: Nucleus
E
Cell viability (fold)
1.2
1.0
0.8
0.6
0.4
0.2
0.0
NS
si-control
si-KIF4 (si-1)
F
HBV infection in PHH (PXB cells)
HBV
si-RNA
72 h
48 h
16 h
15 d
si-RNA
si-RNA
HBV
Wash
Detection
G
HBsAg (fold)
2.0
1.5
1.0
0.5
0.0
***
**
si-control
si-NTCP
si-KIF4 (si-1)
H
Extracellular HBV DNA (fold)
1.4
1.2
1.0
0.8
0.6
0.4
0.2
0.0
***
***
si-control
si-NTCP
si-KIF4 (si-1)
I
KDa
KIF4
150
55
β-actin
si-control
si-KIF4 (si-1)

Fig. 3

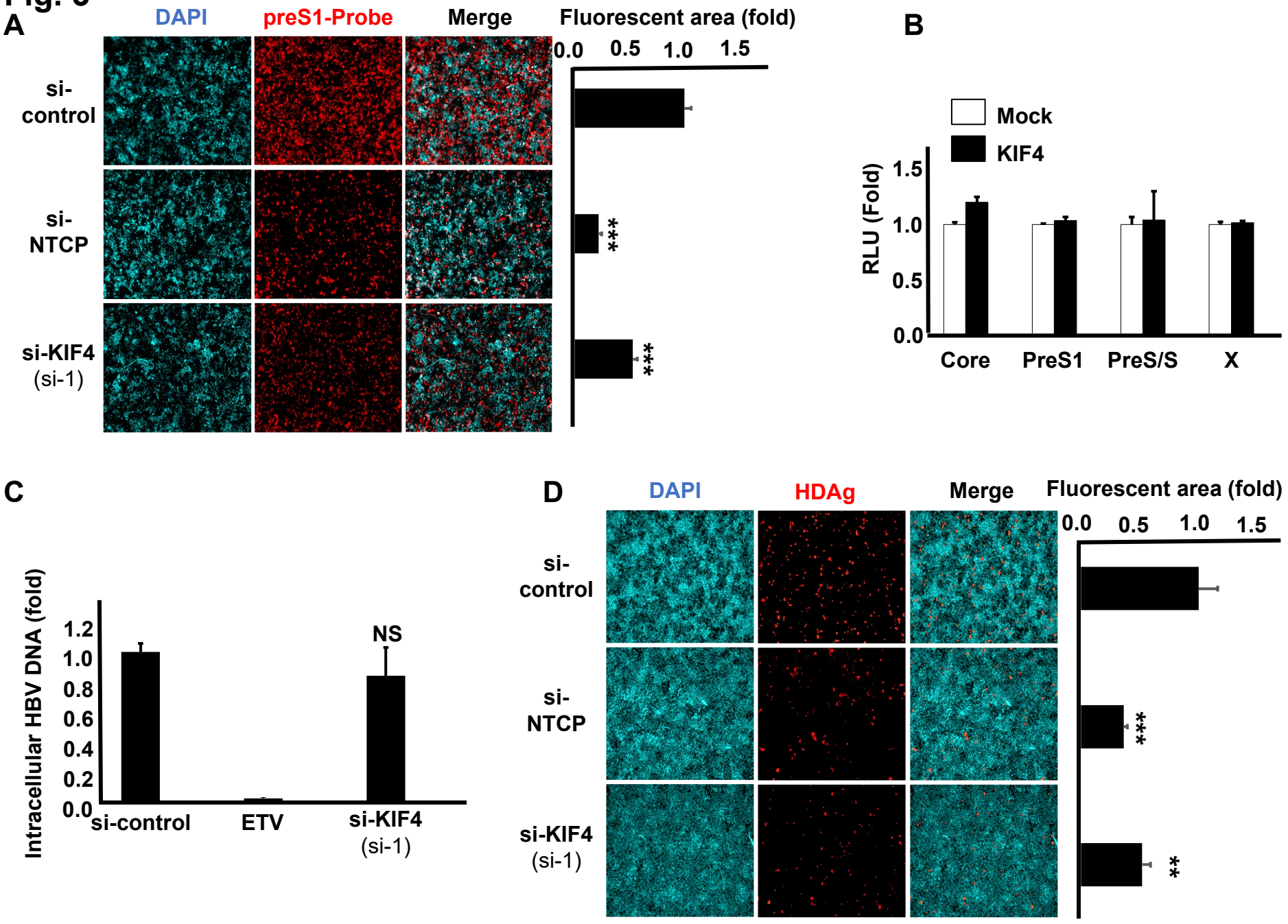
A
DAPI
preS1-Probe
Merge
Fluorescent area (fold)
0.0
0.5
1.0
1.5
si-control
si-NTCP
si-KIF4 (si-1)
***
***
B
Mock
KIF4
RLU (Fold)
1.5
1.0
0.5
0.0
Core
PreS1
PreS/S
X
C
Intracellular HBV DNA (fold)
1.2
1.0
0.8
0.6
0.4
0.2
0.0
NS
si-control
ETV
si-KIF4 (si-1)
D
DAPI
HDAg
Merge
Fluorescent area (fold)
0.0
0.5
1.0
1.5
si-control
si-NTCP
si-KIF4 (si-1)
***
**

Fig. 4

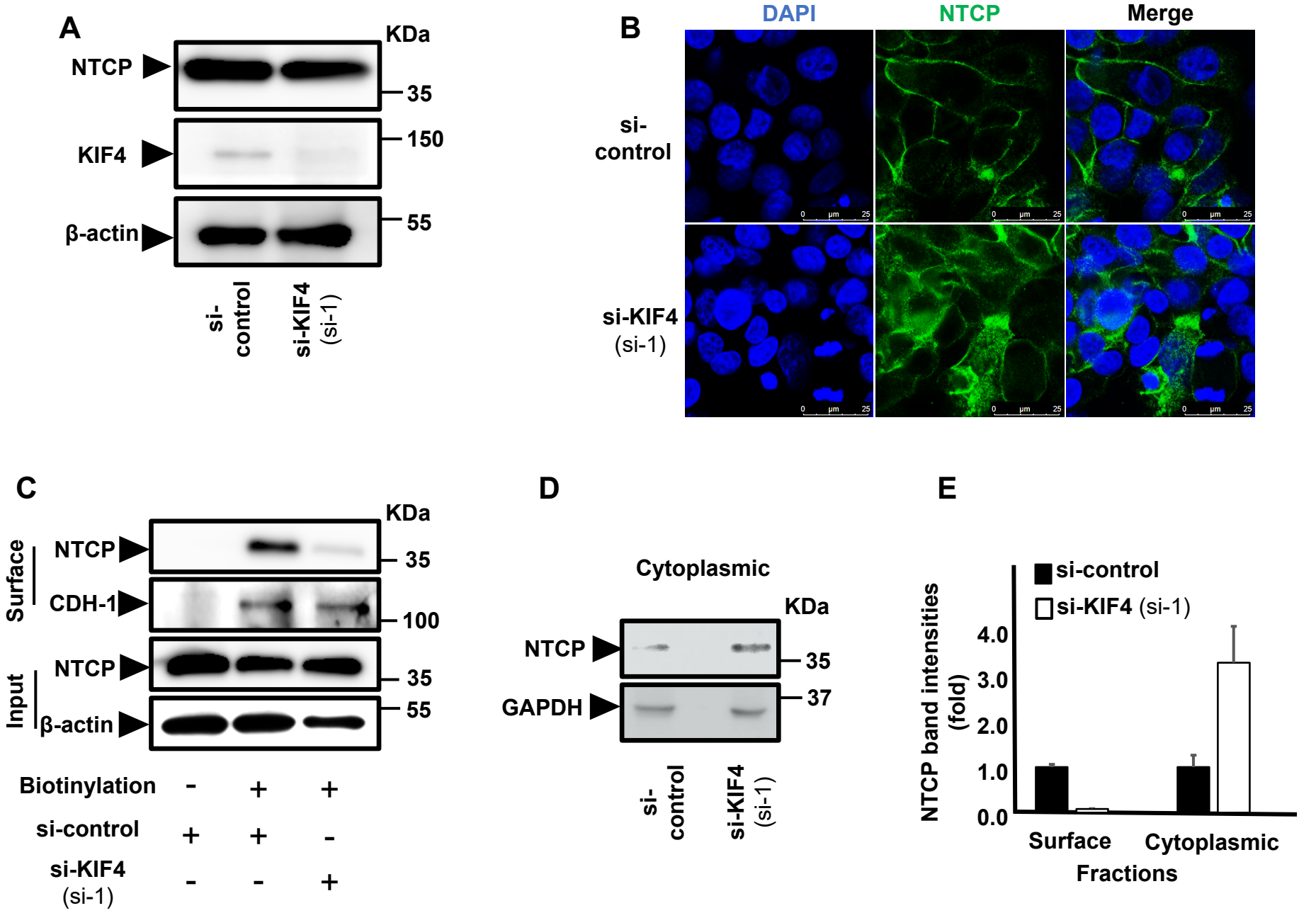
A
KDa
NTCP
35
KIF4
150
β-actin
55
si-control
si-KIF4 (si-1)
B
DAPI
NTCP
Merge
si-control
si-KIF4 (si-1)
C
KDa
Surface
NTCP
35
CDH-1
100
Input
NTCP
35
β-actin
55
Biotinylation - + +
si-control + + -
si-KIF4 (si-1) - - +
D
Cytoplasmic
KDa
NTCP
35
GAPDH
37
si-control
si-KIF4 (si-1)
E
si-control
si-KIF4 (si-1)
NTCP band intensities (fold)
4.0
3.0
2.0
1.0
0.0
Surface
Cytoplasmic
Fractions

Fig. 5

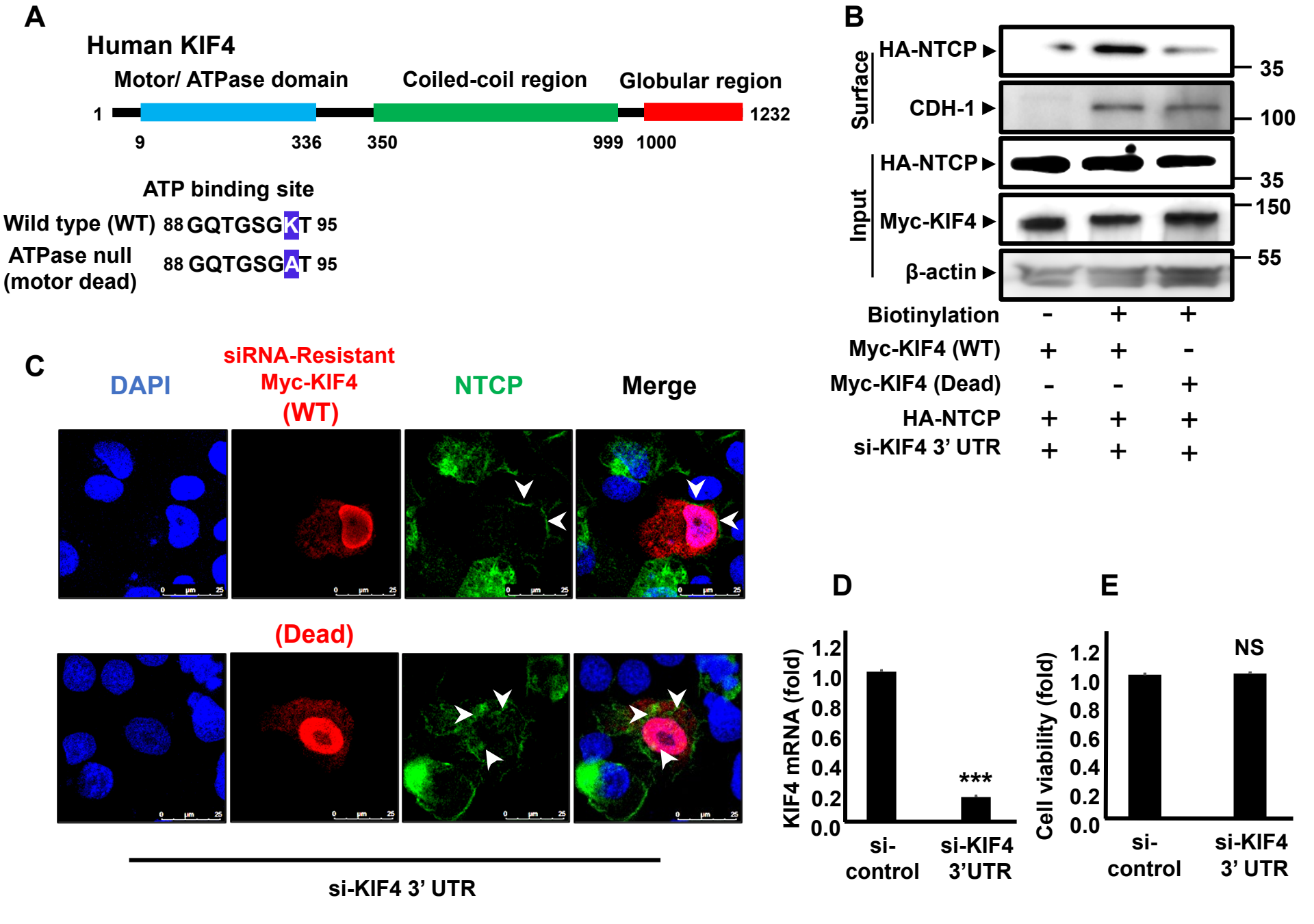
A
Human KIF4
Motor/ ATPase domain
Coiled-coil region
Globular region
1
1232
9
336
350
999
1000
ATP binding site
Wild type (WT) 88 GQTGSGKT 95
ATPase null (motor dead) 88 GQTGSGAT 95
B
Surface
HA-NTCP
CDH-1
Input
HA-NTCP
Myc-KIF4
β-actin
35
100
35
150
55
Biotinylation - + +
Myc-KIF4 (WT) + + -
Myc-KIF4 (Dead) - - +
HA-NTCP + + +
si-KIF4 3' UTR + + +
C
DAPI
siRNA-Resistant Myc-KIF4 (WT)
NTCP
Merge
(Dead)
si-KIF4 3' UTR
D
KIF4 mRNA (fold)
1.2
1.0
0.8
0.6
0.4
0.2
0.0
***
si-control
si-KIF4 3'UTR
E
Cell viability (fold)
1.2
1.0
0.8
0.6
0.4
0.2
0.0
NS
si-control
si-KIF4 3' UTR

Fig. 6

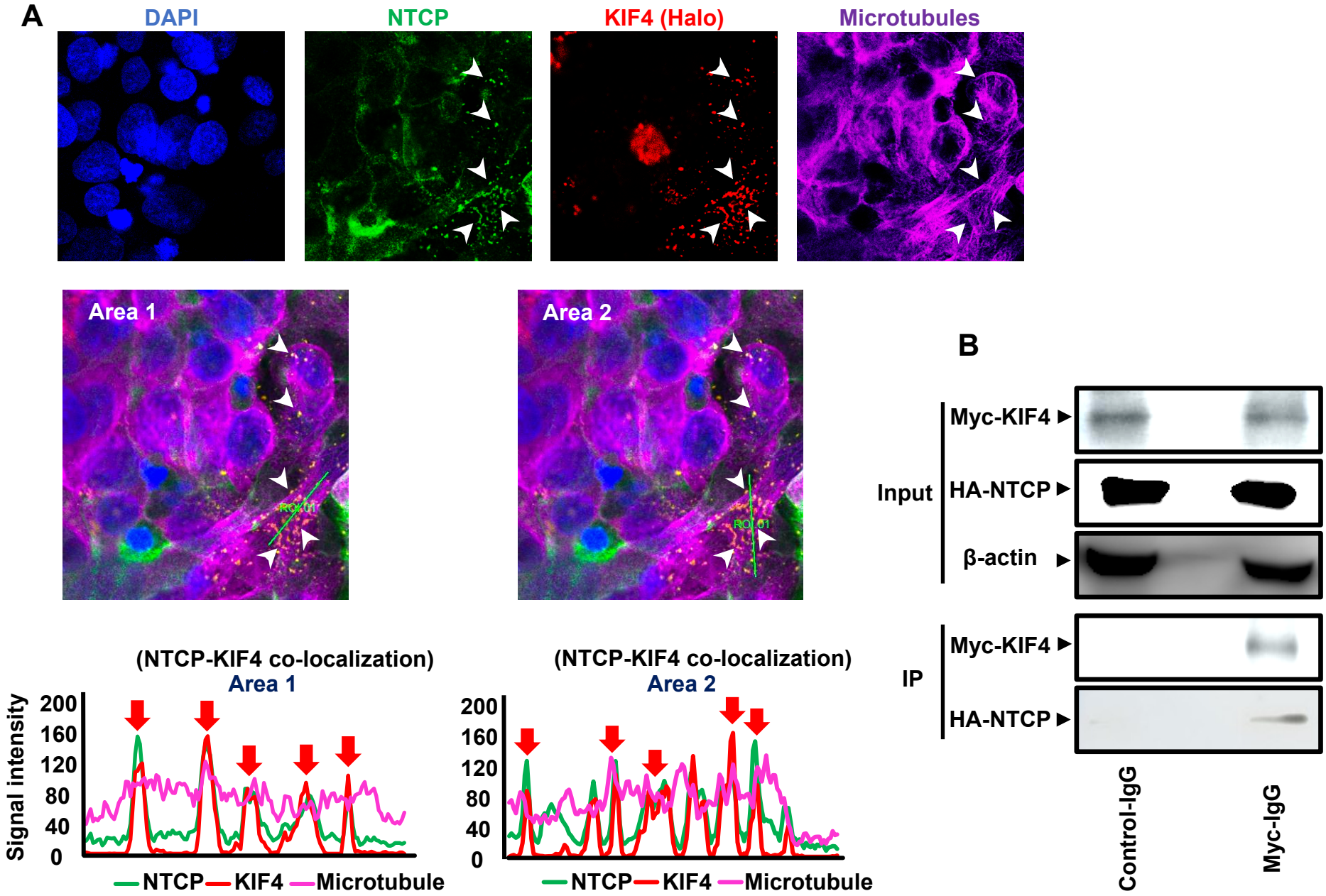
A
DAPI
NTCP
KIF4 (Halo)
Microtubules
Area 1
Area 2
(NTCP-KIF4 co-localization)
Area 1
(NTCP-KIF4 co-localization)
Area 2
Signal intensity
200
160
120
80
40
0
NTCP
KIF4
Microtubule
B
Input
Myc-KIF4
HA-NTCP
β-actin
IP
Myc-KIF4
HA-NTCP
Control-IgG
Myc-IgG

Fig. 7

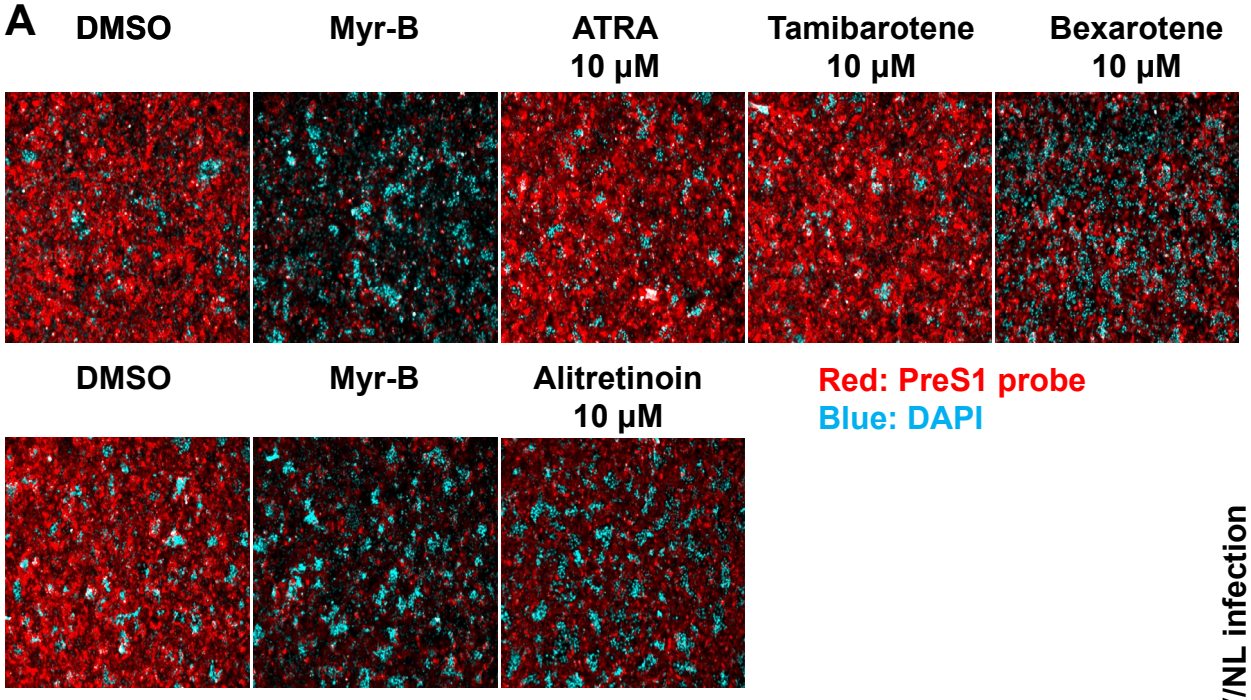
A
DMSO
Myr-B
ATRA
10 μM
Tamibarotene
10 μM
Bexarotene
10 μM
DMSO
Myr-B
Alitretinoin
10 μM
Red: PreS1 probe
Blue: DAPI

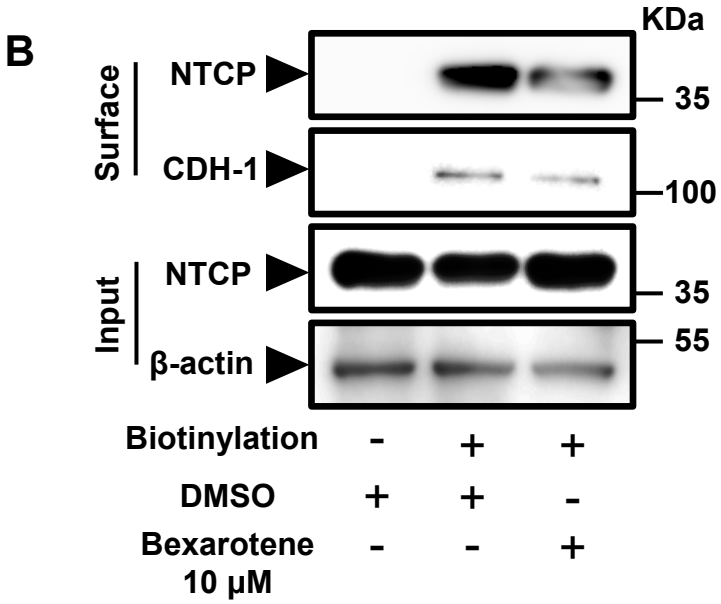
B
KDa
Surface
NTCP
CDH-1
Input
NTCP
β-actin
35
100
35
55
Biotinylation - + +
DMSO + + -
Bexarotene - - +
10 μM

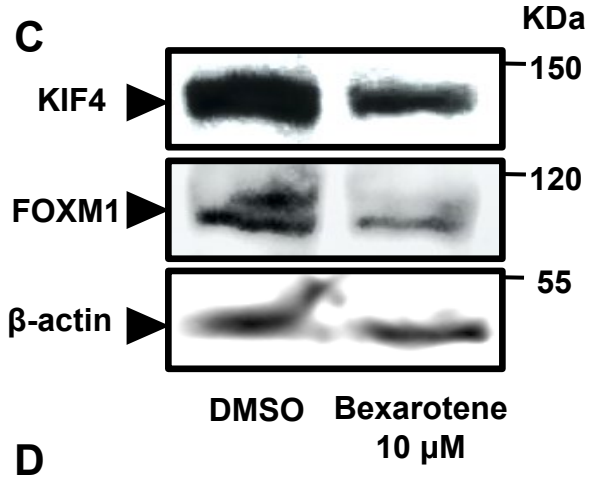
C
KDa
KIF4
FOXM1
β-actin
150
120
55
DMSO
Bexarotene
10 μM

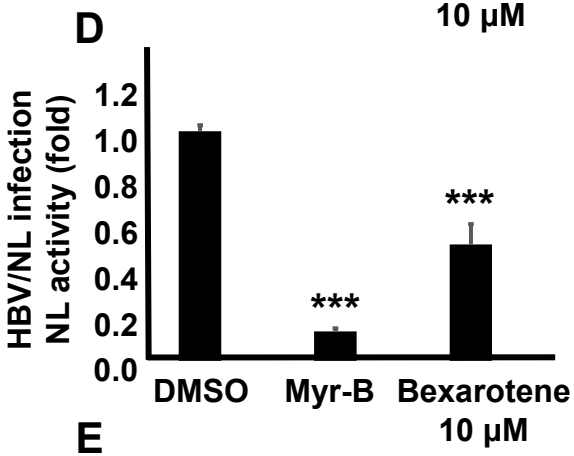
D
HBV/NL infection
NL activity (fold)
1.2
1.0
0.8
0.6
0.4
0.2
0.0
***
***
DMSO
Myr-B
Bexarotene
10 μM

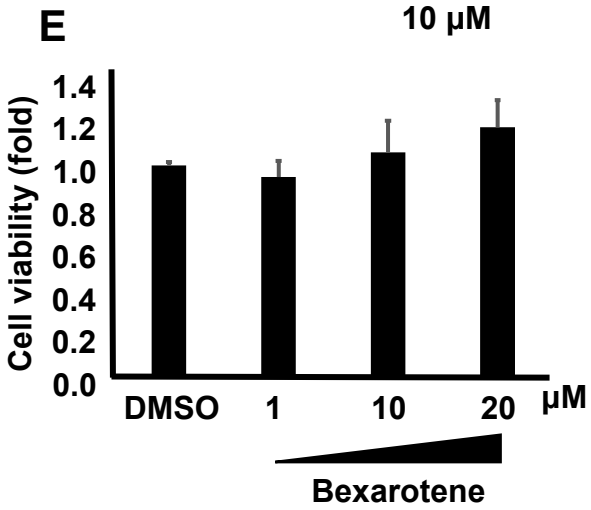
E
Cell viability (fold)
1.4
1.2
1.0
0.8
0.6
0.4
0.2
0.0
DMSO
1
10
20
μM
Bexarotene

Fig. 8

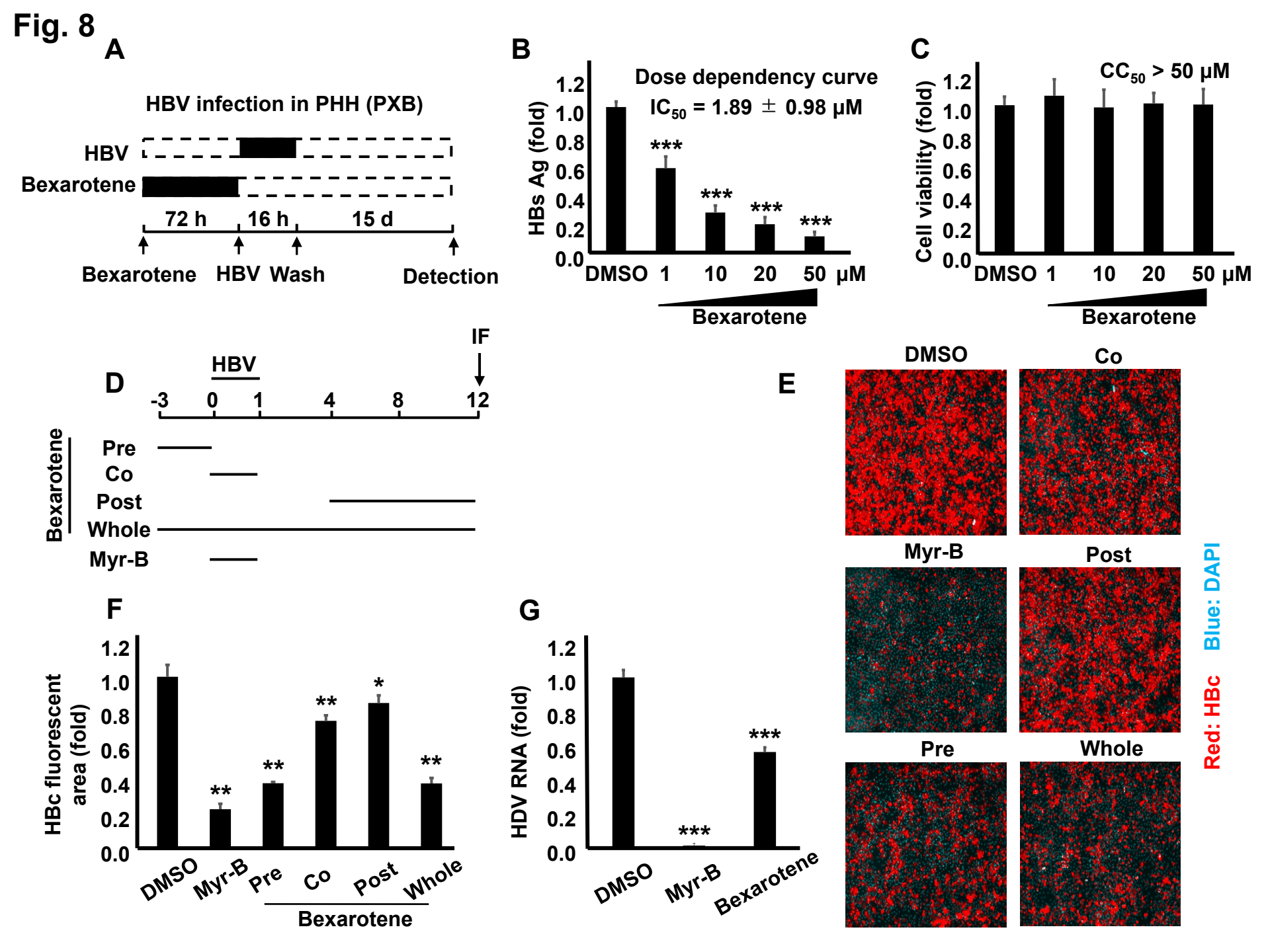
A
HBV infection in PHH (PXB)
HBV
Bexarotene
72 h
16 h
15 d
Bexarotene
HBV
Wash
Detection
B
Dose dependency curve
IC50 = 1.89 ± 0.98 μM
HBs Ag (fold)
1.2
1.0
0.8
0.6
0.4
0.2
0.0
***
***
***
***
DMSO
1
10
20
50 μM
Bexarotene
C
CC50 > 50 μM
Cell viability (fold)
1.2
1.0
0.8
0.6
0.4
0.2
0.0
DMSO
1
10
20
50 μM
Bexarotene
D
IF
HBV
-3
0
1
4
8
12
Bexarotene
Pre
Co
Post
Whole
Myr-B
E
DMSO
Co
Myr-B
Post
Pre
Whole
Blue: DAPI
Red: HBc
F
HBc fluorescent area (fold)
1.2
1.0
0.8
0.6
0.4
0.2
0.0
**
**
**
*
**
DMSO
Myr-B
Pre
Co
Post
Whole
Bexarotene
G
HDV RNA (fold)
1.2
1.0
0.8
0.6
0.4
0.2
0.0
***
***
DMSO
Myr-B
Bexarotene